TECHNISCHE UNIVERSITÄT DRESDEN

Fakultät Umweltwissenschaften

Analytical Models for Plume Length Estimations

Dissertation zur Erlangung des akademischen Grades
Doctor rerum naturalium (Dr. rer. nat.)

vorgelegt von
M. Sc. Prabhas Kumar Yadav

Gutachter:

Herr Prof. Dr. Rudolf Liedl
TU Dresden, Institut für Grundwasserwirtschaft

Herr Prof. Dr. Peter Dietrich
Universität Tübingen, Zentrum für Angewandte
Geowissenschaften-Umwelt- und Ingenieurgeophysik

Dresden, 13. Juli 2012

Erklärung des Promovenden

Die Übereinstimmung dieses Exemplars mit dem Original der Dissertation zum Thema:

„Analytical Models for Plume Length Estimations“

wird hiermit bestätigt.

Dresden,
……..…
Ort, Datum

……..…
Unterschrift (Vorname Name)

Publications from the Thesis

Part of the Chapter 3 is published as:

Liedl, R., P. K. Yadav., and P. Dietrich, (2011), Length of 3D mixing-controlled plumes for a fully penetrating contaminant source with finite width, Water Resour. Res., 47, W08602, doi: 10.1029/2010WR009710

Chapter 4 is submitted for the publication as:

Yadav, P. K., Liedl, R., and P. Dietrich, (2012), Influence of Source Thickness on Steady-State Plume Length, submitted to Water Resources Research.

Chapter 2 is in preparation for submission as:

Yadav, P. K., Händel, F., Liedl, R., and P. Dietrich, (2012), A Brief Review of Contaminated Sites (KORA) Data and of Analytical Models for Plume Length Estimations: Examples of Using Analytical Models for Site Assessment, to be submitted to Grundwasser.

COMITTEE

1. Reviewer:

2. Reviewer:

3. Additional member of the committee:

Day of the defense:

Signature of the head of the PhD committee:

This thesis is dedicated to my parents, M. E. Sugamber Yadav and Mrs. Sarswati Yadav.

Acknowledgements

This PhD was perhaps the second greatest challenge that I have attempted in my life so far. The first one was definitely the failed PhD attempt at Trent University in Canada. I call my PhD a challenge because, for my both attempts, I attempted research on topics that I had absolutely no academic background. I must say that I have been lucky to get two opportunities in life and for that, I have to thank quite many people and organizations.

Most important, of course, was the funding agency- IPSWAT, which did not only provide me with a basic salary for three years but it also provided funds for my academic trip to Prof. Charles Werth, University of Illinois, USA and for several academic conferences and field trips. Thank you IPSWAT (Mrs. Cornelia Parisius, Mrs. Gabriele Al-Khinli and Ms. Sara Sabzian) and German Ministry of Eduction and Research (BMBF).

I must say that I had the best PhD supervisors in the world. I strongly doubt that there can be a mentor better than Prof. Rudolf Liedl- a perfect human being. I specially enjoyed his, difficult to understand, mathematical jokes. My second supervisor, Dr. Peter Dietrich, not only connected me to one of the premium environment sector research institute of the world (Helmholtz-Centre for Environmental Research-UFZ) but he also has been the guiding **force** behind my every works, every academic trips, every publications. Thank you Prof. Liedl and thank you Dr. Dietrich.

I am thankful to every one from my Institute, (IGW, Chief: Prof. Liedl), for bearing me at times and supporting me at other times. Thank you, Dr. Michael Dietze, Dr. Diana Burghardt, Dr. Guilermo

De Aguinaga, and very soon to become Dr.- Thomas Reimann, Marc Walther, Norbert Böttcher and Falk Händel. My special thanks to Ms. Nancy Reimann, secretary at my institute, for clearing all my administrative paper works and specially for speaking in English with me. I also thank students who worked with me at IGW, specially M. Sc. Jianfeng Xu, M. Sc. Christian Müller, M. Sc. Johana Grajales, M. Sc. Bijendra Man Bajracharya and M. Sc. Juan Peña for letting me learn from their M.Sc. thesis works.

Definitely, this PhD, or anything I have achieved in my life, would have not been possible without blessings from my parents, M. E. Sugamber Yadav and Mrs. Sarswati Yadav. I must also thank my wife, Mrs. Anu Yadav, for supporting me and showing incredible patience and understanding through-out the PhD works. Lastly, my little daughter, Ms. Arya Yadav, born on 14.03.2011 deserves a special mention for just being what she is.

Prabhas Kumar Yadav

Thesen

1. Review of Contaminated Site Data

The compilation, analyses and post-processing of the sufficiently large contaminated site database can provide information that can be decisive in the assessment of an unknown or a new site. Moreover, these compilations can provide estimate of parameters, which are very difficult to measure or of those that cannot be directly measured, that can be used for modeling and prognosis purposes.

2. Review of Analytical Models

Analytical models are most often used to verify the accuracies of numerical models, which are mostly developed for the analysis of complex systems. More often these analytical models are simple algebraic equations and therefore, they can be used for rapid estimation of parameters that are important for the pre-assessment of contaminated sites (for example) or to get initial input parameters for the numerical models. A good knowledge of these analytical models can significantly simplify complex analysis.

3. Contaminant Plume Length Estimations

Contaminant plume lengths specify how far contaminants will travel downgradient of their source. Any possibility for a good estimate of this parameter can largely simplify the assessment of the contaminated sites. Of particular importance is the maximum length of the contaminant plume. An assessment is necessary, because the remediation of

contaminated sites is generally very expensive and not every site requires remediation.

4. Development of 3D-Analytical Models for Plume Length Estimation

Only very few 3D analytical models for plume length estimations can be found in literature. This is largely due to fact that analytical solutions of complex scenarios, e.g., normal field conditions, are very often not obtainable. While simplifications of field condition can lead to a development of a 3D analytical model, but the applicability of the developed model can be very restrictive. A 3D model is more realistic, but a balance between simplifications of field condition and its applicability has to be considered.

5. Development of Simple Numerical Techniques for Plume Length Estimation

In general, numerical techniques are expensive and often time consuming method that are used for contaminant plume length estimations. But if simple numerical techniques can be developed, then limitations of using numerical methods and also the restrictions of the analytical models can be overcome.

Thesen

1. Daten-Review zu Kontaminationsstandorten

Die Zusammenstellung, Analyse und die Nachbearbeitung der im Umfang ausreichenden Daten zu den Kontaminationsstandorten kann Informationen geben, die maßgebend für die Bewertung eines unbekannten oder neuen Standorts sein kann. Darber hinaus kann diese Zusammenstellung Hinweise zu Parametern bieten, welche für Modellierungs- und Prognosezwecke genutzt werden können.

2. Review analytischer Modelle

Analytische Modelle werden oft genutzt um die Genauigkeit von numerischen Modellen zu verifizieren, welche oft für die Analyse von komplexen Systemen entwickelt werden. Zumeist sind diese analytischen Modelle simple algebraische Gleichungen, was eine schnelle Bestimmung von Parametern mit Relevanz für die Vorabschätzung von kontaminierten Standorten (zum Beispiel) und die Gewinnung von Eingangsparametern für die numerische Modellierung ermöglicht. Eine zuverlässige Kenntnis dieser analytischen Modelle kann signifikant komplexe Analysen vereinfachen.

3. Abschätzung der Schadstofffahnenlängen

Schadstofffahnenlängen bestimmen wie weit Schadstoffe stromabwärts ihrer Quelle transportiert werden. Jedwede Möglichkeit einer guten Abschätzung dieses Parameters kann die Bewertung des Kontaminationsstandortes stark vereinfachen. Besondere Wichtigkeit kommt der

maximalen Schadstofffahnenlänge zu. Eine Abschätzung ist notwendig, da die Sanierung an kontaminierten Standorten generell sehr kostspielig ist und nicht grundsätzlich jeder Standort einer Sanierung bedarf.

4. Entwicklung eines dreidimensionalen analytischen Modells zur Fahnenlängenabschtzung

Es konnte nur eine geringe Anzahl an dreidimensionalen analytischen Modellen für die Fahnenlängenabschätzung in der Literatur gefunden werden. Dies gründet auf dem Fakt, dass analytische Lösungen von komplexen Szenarien, z.B. typische Feldbedingungen, oftmals nicht möglich sind. Obwohl die Vereinfachung von Feldbedingungen zur Entwicklung von dreidimensionalen analytischen Modellen führen kann, ist die Anwendbarkeit dieser Modelle sehr eingeschränkt. Ein 3-D Modell ist deutlich realistischer, jedoch muss ein Mittelweg zwischen Einfachheit der im Modell berücksichtigten Feldbedingungen und der Anwendbarkeit gefunden werden.

5. Entwicklung einer simplen numerischen Methode zur Fahnenlängenabschätzung

Zumeist sind numerische Methoden kostenintensiv und oft zeitaufwendig, wenn sie zur Schadstofffahnenlängenabschätzung genutzt werden. Bei der Entwicklung von simplen numerischen Methoden können jedoch die Limitierungen bei der Nutzung numerischer Methoden und die Einschränkungen der analytischen Modelle überwunden werden.

Abstract

This thesis dealt with the techniques that could be used for the pre-assessment of contaminated sites. The goals of the thesis were based on a simple fact that every contaminated site possesses certain potential to degrade natural resources, specifically groundwater and land resources. The thesis focused on using mathematical and statistical techniques to predict the maximum length of contaminated plumes or L_{max}, which it considered as a key parameter that could be used for the site assessment.

As the first thesis work, data from KORA sites were compiled and analyzed. From the analyses, it was found that the L_{max} for BTEX plumes are in average under 150 m long. Further, for this work, Analytical Models that can be used to estimate L_{max} were reviewed and, examples comparing model and field L_{max} were presented.

The second work for the thesis focused on a development and analysis of a new 3D-analytical model for a finite planar and fully penetrating source. An implicit expression for predicting L_{max} was obtained. The analysis of the developed model suggested that the longest L_{max} will result if the source takes an approximately square shape.

The last part of the thesis improved the 3D-analytical model obtained in the second work by presenting an expression for a finite planar source that only partially penetrates the aquifer. For this work, a very simple numerical technique was developed that not only simplifies numerical analysis of the scenarios considered in this thesis but it also bears potentials to be used for very complex subsurface reaction transport scenarios.

This thesis has been successful in narrowing research-gaps on problems related to contaminated sites management.

Kurzfassung

Diese Doktorarbeit befasste sich mit Methoden, welche für eine Vorabbewertung von kontaminierten Standorten genutzt werden können. Die Ziele der Arbeit basierten auf dem einfachen Fakt, dass jeder kontaminierte Standort ein bestimmtes Potential besitzt, natürliche Ressourcen, speziell Grundwasser- und Bodenressourcen, in ihrer Qualität negativ zu beeinträchtigen. Die Arbeit war auf die Nutzung mathematischer und statistischer Techniken zur Abschätzung der maximalen Schadstofffahnenlänge, auch L_{max}, fokussiert, welche als entscheidender Parameter für die Standortbewertung genutzt werden kann.

Der erste Teil der Doktorarbeit beinhaltete die Zusammenstellung und Analyse von Daten einer Vielzahl von KORA-Standorten. Anhand dieser Untersuchungen konnte festgestellt werden, dass L_{max} von BTEX-Fahnen im Mittel unterhalb von 150 m liegt. Des Weiteren wurden für diese Arbeit analytische Modelle, welche für die Abschätzung von L_{max} genutzt werden können, kritisch bewertet und vergleichende Beispiele zwischen mit Modellierung bestimmter und im Feld ermittelter L_{max} präsentiert.

Der zweite Teil der Doktorarbeit zielte auf die Entwicklung und Analyse eines neuen dreidimensionalen, analytischen Models für eine finite, planare und über die komplette Mächtigkeit vorherrschende Quelle ab. Es konnte ein impliziter mathematischer Ausdruck zur Vorhersage von L_{max} gewonnen werden. Die Analyse des Models wies darauf hin, dass maximale L_{max} erreicht werden, wenn die Quelle eine annähernd quadratische Form aufweist.

Der letzte Teil der Doktorarbeit diente der Weiterentwicklung des dreidimensionalen, analytischen Modells aus dem zweiten Teil durch die Entwicklung eines Ausdrucks für eine finite, planare Quelle, welche jedoch nur teilweise die Mächtigkeit des Grundwasserleiters kontaminiert.

Für diese Arbeit wurde ein sehr einfacher numerischer Ansatz entwickelt, welcher die numerische Analyse der in dieser Arbeit berücksichtigten Szenarien nicht einfach nur erleichtert, sondern auch das Potential beinhaltet diesen auf komplexe, reaktive Transportszenarien im Untergrund anzuwenden.

Abschließend kann gesagt werden, dass diese Arbeit erfolgreich zur Verringerung von Forschungslücken in der Problematik des Managements kontaminierter Standorte beigetragen hat.

Contents

List of Figures

List of Tables

Chapter 1

Introduction

In a very broad sense, a contaminated site can be defined as a site that has been altered from its original and natural chemical condition. Henceforth, a contaminated site can also result from natural phenomena, e.g., flood, volcanic eruption. However, more important are those that have resulted from human interventions. Of particular importance are the fuel and industrial waste storage sites, mostly because these (storage) sites are crucial for sustaining modern human lifestyle. With rapid industrialization, especially in developing countries with large population, such as China, India, the number of contaminated sites are definitely to rise by several folds in coming years. Combining weak environmental regulations and increased number of sites can lead to higher stresses in maintaining healthy population and meeting the demand for useful natural resources. While stricter regulations can limit the increase of new sites, the containment of the large number of existing sites is still a very big challenge. A study by *Prokop et al.* (2000) provides an estimate of contaminated sites in different countries of European Union (EU); among which more than 400,000 sites are estimated to exist in Germany. While the direct impacts of contaminated sites to human population have been almost contained in Germany and in most of the other developed nations, the problem related to their impacts on natural resources remains largely unresolved. Several research projects, e.g., KORA (Germany), CORONA (EU), have targeted issues related to management of contaminated sites, but these efforts have not been conclusive. Thus, more dedicated efforts are required. This thesis is intended to narrow the knowledge gaps on a proper management of contaminated sites, especially of fuel storage sites where contaminants have reached the saturated zone of the aquifer. In this chapter, a general information on contaminated sites and their management, e.g., processes active at contaminated sites, contaminated sites assessment tools, are provided. Towards the end of the chapter, the scope of the thesis is outlined.

1.1 Active Processes at Contaminated Sites

A simplest contaminated site can still be very complicated to understand. This is largely due to combination of different processes active at contaminated sites at any instant. Broadly, these different processes can be classified into three main categories: the physical processes, the chemical processes and the biological processes. To begin with, it is physical processes- infiltration and percolation that lead to transport of contaminant to the groundwater. Infiltration is driven by gravitational force and capillary force, with the latter force resulting in a so-called residual contamination of the unsaturated or vadose zone of the aquifer. Eventually, under gravitational force contaminants percolates to the saturated or phreatic zone. The behavior of contaminants after reaching the saturated zone depends upon its chemical properties. Hydrophobic contaminants or Non-Aqueous Phase Liquids (NAPL) tend to either remain above the water surface in the case of Light Non-Aqueous Phase Liquid (LNAPL), e.g., fuel hydrocarbons such as Benzene, Toulene, Ethylbenzene, Xylene or BTEX, or they tend to settle at the bottom of the aquifer in the case of Dense Non-Aqueous Phase Liquid (DNAPL), e.g., industrial solvents such as vinyl chloride, di, tri or tetra cholorethene. On the other hand, hydrophilic contaminants- mostly inorganic contaminants, e.g., lead, arsenic, tend to uniformly mix with water. A schematic contaminant site scenario is provided in Figure 1.1. As contaminant or Electron Donor (ED) enters the saturated zone, it is flown downgradient due to advective or groundwater flow (v). From its flow paths, contaminant disperses due to dispersive processes, both mechanical dispersion (largely, a function of v and the packing of porous medium in the aquifer) and molecular diffusion (a function of concentration gradient). The dispersive processes bring ED in contact with other chemicals originally present in the groundwater. Of particular interest are a group of compounds, called Electron Acceptors or EA, that are reactive to ED. Most important among the EA are O_2, NO_3, SO_4. The reaction between the EA and ED, the main chemical process, are catalysed by the microorganisms e.g., *Thullner et al.* (2002), *Wiedemeier et al.* (1999), which makes biological processes, arguably, the key process in degradation and movement of the contaminant. Physio-chemical processes such as adsorption and absorption also hinder the downgradient movement of the contaminant. Beside, comparatively less important physical processes such as volatilization, dilution etc. may also be active at contaminated sites (e.g., *Wiedemeier et al.*, 1999).

In general, at every contaminated sites some combinations of the different processes discussed above, which lead to degradation of contaminants or ED, are naturally and always active. Hence, a term Natural Attenuation (NA) has been introduced and it has been legally defined in USA (see, *EPA* (1999)) as:

"The natural attenuation processes that are at work in such a remediation ap-

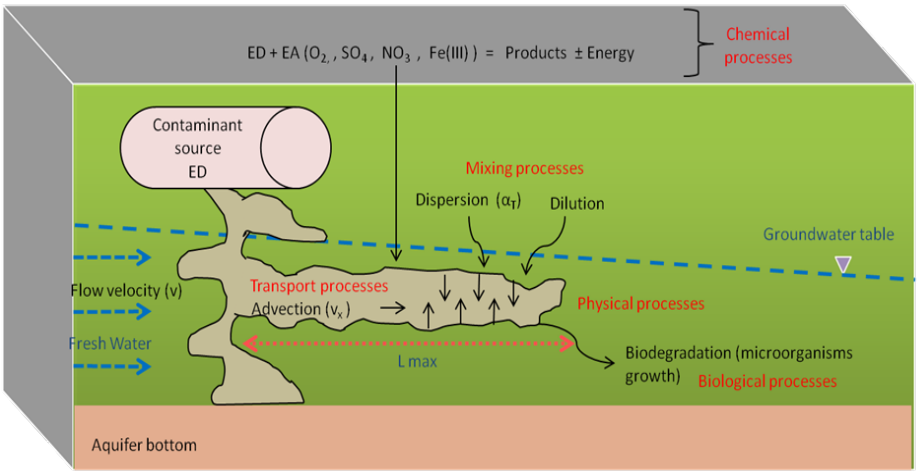

Figure 1.1: A general contaminated site scenario

proach include a variety of physical, chemical, or biological processes that, under favorable conditions, act without human intervention to reduce the mass, toxicity, mobility, volume, or concentration of contaminants in soil or groundwater."

In Germany, *LABO* (2009) provides the following definition for NA:

"Natürliche Schadstoffminderungsprozesse sind biologische, chemische und physikalische Prozesse, die ohne menschliches Eingreifen zu einer Verringerung der Masse, der Fracht, der Toxizität, der Mobilität, des Volumens oder der Konzentration eines Stoffes im Boden oder Grundwasser fuhren. Zu diesen Prozessen zählen biologischer Abbau, chemische Transformation, Sorption, Dispersion, Diffusion und Verflüchtigung der Stoffe."

Stages of Contaminant Plume Development

Development of a contaminant plume is a step-wise process. *Rugner and Teutsch* (2001) provide very concise details on the development of the contaminant plume (see Figure 1.2). During the first stage or t_1 (in Figure 1.2), there is essentially no decay of the contaminant and the plume rapidly spreads. Degradation processes (chemical, physio-chemical and biological) leading to loss of contaminant from the groundwater begin in the second stage or t_2. The biological degradation process, which is often the most important degradation process, may only begin a few months after the t_1 stage. The degradation processes impede the rapid spread of contaminant and a steady-state condition (the t_3 stage), in which degradation processes equals the spread of the contaminant, is attained. Depending upon the

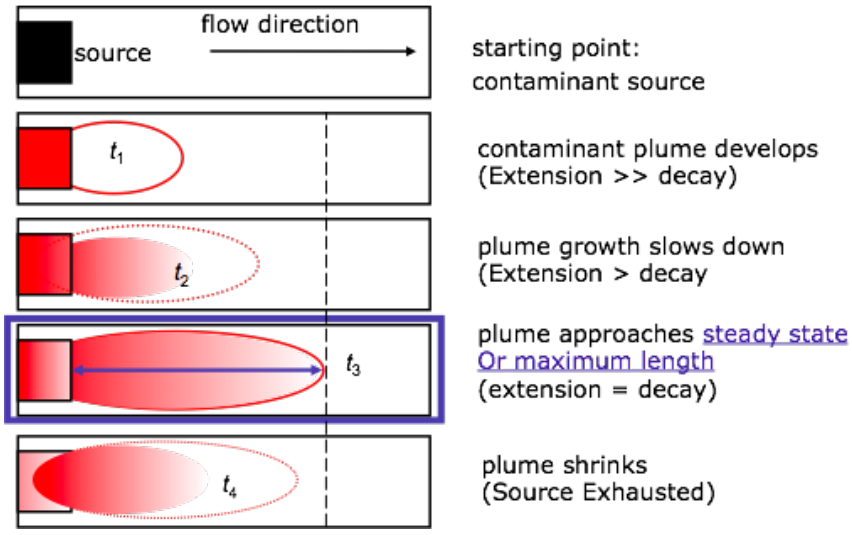

Figure 1.2: Development of a contaminant plume. Modified from *Rugner and Teutsch* (2001)

bio-geo-chemical properties of the aquifer, the t_3 stage may be reached after a few years or even a decade after the t_2 stage. The t_3 stage, at which the plume has reached the maximum spread in all directions, can last as long the continuity of the contaminant mass and flow remains unchanged. The plume will eventually start shrinking when the stage t_4 is reached, pointing that the contaminant source has begun to get exhausted.

From the site management perspective, the t_3 stage is the most important stage of all stages of the plume development. This is largely because, it is at this stage the maximum spread of the contaminant is realized and also because, this stage may have the longest time span. The focus of this thesis is also on the t_3 stage or of the plume that is at the steady-state. Next, the methods for managing contaminated sites are introduced.

1.2 Contaminated Sites Management

Every contaminated site possesses different but certain risk to natural resources. As such an ideal site management method is required to be very flexible and inclusive. Applying an appropriate active remediation technique (e.g., *EPA* 2000) may be an ultimate solution in the management of contaminated sites. However, these techniques are in general expensive and considering the number of existing sites, applying them to all sites may be impractical if not impossible. As was discussed in

section 1.1, some form of natural attenuation is always active at all contaminated sites, therefore the management procedure must include a risk-based assessment tool for first categorizing (pre- assessment) the sites and later, providing a decision tool for selecting an appropriate remediation technology. This thesis deals with techniques that can be adopted for the pre-assessment of contaminated sites, hence field based active remediation techniques are omitted from the subsequent discussions.

Obtaining a good estimation of a steady-state (or maximum) length of the plume (L_{max}) can serve as a suitable indicator for the pre-assessment of a contaminant site. A decision criterion can be based on risk that L_{max} possesses to a receptor (human or natural resources). This leads to a key question that this thesis will attempt to answer, and that is, "how to easily estimate L_{max} ?" Due to high costs involved in obtaining field data, an appropriate pre-assessment tool should require only few parameters, from which it should be able to provide a good estimate of L_{max}. Computational techniques that can be used for estimating L_{max} is very briefly introduced below.

Computational Techniques for Estimating L_{max}

Numerical and analytical modeling are the two very general computational techniques that are applied for estimating L_{max}. Comparatively, numerical models are more often used for analyzing contaminant transport scenarios, including for the estimation of L_{max}, than analytical models. These (numerical) models have been in continuous development since the late 70's of the last century, and by now several free numerical codes, such as PHT3D (*Prommer et al.*, 2003), MIN3P (*Mayer*, 1999), as well as commercial algorithms, such as FEFLOW, HYDRUS, are available. Numerical models discretizes the model domain into smaller units, and they solve the algebraically transformed solute transport equation (Advection-Dispersion-Reaction (ADR) equation) at each discrete points or units. Any combination of boundary conditions or constraints within the domain, e.g., multi-species reaction, complex reaction mechanisms, can be simulated using these models so long appropriate discretization of the domain can be achieved and that powerful computing machines are available. Details on the modeling techniques and capabilities of numerical models can be found in standard texts, e.g., *Zheng and Bennett* (2002), *Bear and Cheng* (2008). Although numerical models are flexible, they still require large number of field parameters to provide a good estimate of the actual plume. In general, using numerical models for obtaining L_{max} can be expensive, they may require higher user expertise and longer simulation time.

In contrast to numerical models, analytical models are often simple algebraic expressions providing L_{max} explicitly as a function of few field parameters. These

models generally simplify the actual field conditions by making several assumptions such as homogeneous domain, uniform flow, and simple reaction mechanisms. L_{max} is then derived for the simplified domain by analytically solving the ADR equation. The drawback due to simplification of the actual domain is expected to overestimate L_{max}, which can still be acceptable in many cases. Analytical models, for estimating L_{max}, have been in development since the 60's of the last century (see for e.g., *Wexler*, 1992). The earliest models were generalized by *Domenico and Robbins* (1985) and *Domenico* (1987), which have been further improved by several authors in recent years, e.g., *Ham et al.* (2004), *Liedl et al.* (2005), *Liedl et al.* (2011). Due to simplicity and requirement of few field parameters, analytical models provide a very strong alternative to other methods for the pre-assessment of contaminated sites.

1.3 The Scope of the Thesis

It is rather impossible to completely understand a contaminated site. This is largely due to multi inter-related processes active at any site at all times. Rather than attempting to understand a site, this thesis will attempt to provide tools that can be useful for the pre-assessment of the contaminated sites. As such, in addition to the scientific goals, the thesis also targets the management aspects of the contaminated sites. The thesis considers L_{max} as a key parameter that can be used for the pre-assessment of the contaminated sites and so, focus are on exploring several aspects of that parameter. More concisely, the following points are outlined as the scope of the thesis:

1. Reviewing and analyzing contaminated sites data and analytical models that can be used for estimating L_{max}.

2. Development of a 3D analytical model for estimating L_{max} for a fully penetrating contaminant source.

3. Improvement of analytical model for estimating L_{max} for a partially penetrating contaminant source.

The chapters of the thesis are organized in the following way: In chapter 2 data from the KORA sites are collected, analyzed and summarized. Further in that chapter, a brief review is made of the analytical models that can be used for the assessment of the contaminated sites. This chapter also includes examples on using analytical models for calculating and comparing L_{max}. Chapter 3 will introduce to a development of a 3D analytical model for a fully penetrating source, from which estimation of L_{max} will be made. The developed model will be used

to explore the impacts of several field parameters on the L_{max}. In the fourth chapter, the analytical model developed in chapter 3 will be modified to fit to the partially penetrating source. In this chapter evaluation of L_{max} provided by analytical models are made using numerical experimentations. Recommendations for future works are provided in the last chapter of the thesis.

Chapter 2

A Brief Review of Contaminated Sites (KORA) Data and of Analytical Models for Plume Length Estimations: Examples of Using Analytical Models for Site Assessment

2.1 Introduction

[1] Some form of natural degradation of contaminants are always active at every contaminated sites (*Wiedemeier et al.*, 1999). The degradation results, largely, due to combination of physical processes (diffusion, dispersion), chemical processes (reactions between reactants, e.g., a redox reaction between an Electron Donor (EA) and an Electron Acceptor (EA)) and biological processes (mostly catalyzing the chemical processes). As degradation of contaminants results, a term Natural Attenuation (NA) has been introduced and defined as a possible method of site remediation. In Germany NA has been defined by *LABO* (2009) as, "Natürliche Schadstoffminderungsprozesse sind biologische, chemische und physikalische Prozesse, die ohne menschliches Eingreifen zu einer Verringerung der Masse, der Fracht, der Toxizität, der Mobilität, des Volumens oder der Konzentration eines Stoffes im

[1] The German translation of this chapter is to be submitted to Grundwasser Journal

Boden oder Grundwasser fuhren. Zu diesen Prozessen zählen biologischer Abbau, chemische Transformation, Sorption, Dispersion, Diffusion und Verflüchtigung der Stoffe." Common contaminants such as different petroleum constituents, solvents etc., are slower in degrading naturally, hence a term Monitored Natural Attenuation (MNA) is often used as a substitute for NA when degradations are to be monitored for a longer time. NA has a significant role for the management of contaminated sites, largely, because it is rather impractical if not impossible to actively remediate a very large number (e.g., see *Prokop et al.*, 2000) of sites that are estimated to exist in Germany, European Union (EU) and elsewhere. Even if no remediation works are to be done, it is still very important to assess every site for the risk it possesses to the human being, animals and natural resources. Any assessment work relates to understanding of NA at the contaminated site. With only monitoring costs involved and practically very little or no adverse environmental impacts, considering NA as a remediation technique after the assessment of the sites is possibly the best scenario for the site owners or regulating agencies.

As microorganisms play the catalyzing role in the natural degradation of contaminants, the optimum conditions for their growth and functions are pre-requiste for a stronger NA. Several research works, for e.g., *Huang et al.* (2003), *Thullner et al.* (2002), have experimentally and numerically shown that microbial population and consequently the contaminant degradations are predominantly concentrated at the edge of the plume. Besides position in the domain, the optimum conditions for microorganisms are also related to physical parameters such as dispersivities and conductivities in all spatial directions. Transverse dispersivities, in particular, have been shown to control mixing among the reactants in several research works, for e.g., by *Grathwohl et al.* (2001) or *Cirpka* (2002). Longitudinal dispersivity, on the other hand, has an ignorable role (*Liedl et al.*, 2005, *Huang et al.*, 2003 etc). *Norris* (1995) suggests that the aquifer matrix with hydraulic conductivity (K) greater than $10^{-6} - 10^{-4}$ cm/sec is only capable of transporting microorganisms in aquifers. *Norris* (1995) also suggest that, apart from hydraulic conductivity, mineralogy and sediment structure of the aquifer matrix can also affect microorganisms movement in the aquifers. Microorganisms are also selective to among different EA found in aquifer. This leads to a sequential decay of EA in aquifer. Due to highest redox potential of an oxygen partnered reaction, and to similar extent of nitrates, any role of other EA's are only likely when oxygen (or nitrates) is completely exhausted from the system. In general, several site parameters are required to be collected before a proper decision on the assessment of a site can be made.

In recent years several large scale NA related research projects, such as CORONA (EU), Underground Storage Tank (UST) related projects by Environmental Protection Agency- USA to name few, have been initiated or concluded. Very recently, a German Federal Ministry of Education and Research (BMBF) funded priority

project "Kontrollierter natürlicher Rückhalt und Abbau von Schadstoffen bei der Sanierung kontaminierter Grundwässer und Böden" (KORA) was completed. The results compiled from these large scale field projects provide a reasonably large database of different parameters that are active at sites that are undergoing NA. *Wiedemeier et al.* (1999) has analyzed several such database, including data from a very extensive field investigation of airfield sites in USA. Likewise, *Teutsch et al.* (1997) analyzed data compiled from several literatures. Techniques, e.g., numerical or analytical modeling, that are used for site assessment are very heavily dependent upon these data studies for estimating parameters, for example estimating different dispersivities.

The steady-state plume length, which translates to the maximum possible extension of contaminant in the direction of flow (L_{max}), can be one of the key parameters knowing which can lead to a robust assessment of a contaminated site. Numerical models have been commonly used for predicting plume lengths and L_{max}. Although very flexible in applications, these numerical models usually require powerful computers and a high level of expertise for applying them. In addition, a very large initial information on several parameters may be required. Analytical models, which are more often a simple algebraic equation, can be a good alternative to numerical models for estimating L_{max}. These analytical models have been in development since the 60's of the last century (see, *Wexler*, 1992), and several of them capable of handling different site conditions are now available in literature. Still the applicabilities of these models are limited due to much larger variations observed in field. The limitations are largely due to simplifying assumptions, e.g., a homogeneous system when the field is generally heterogeneous, made in the formulation of these models. These limitations should result in overestimation of the actual plume conditions, but only very few research works (e.g., *Newell et al.*, 1995) have compared field and analytically estimated plume lengths for more than two different sites. Contaminated sites are often isolated and abandoned and therefore they have very little economical value. Both NA and analytical models are economical tools and can be utilized to manage less-worthy and abandoned sites. Unfortunately, scientific applicability and confidence in utilizing these techniques are rather limited. A major part of this research work focuses on analytical models that can be used to explain NA at sites.

This chapter is arranged in the following way: In the first part, data available from different KORA reports are tabulated and analyzed. Data analyses are primarily focused on plume length. The second part of this chapter reviews analytical models for predicting plume lengths undergoing NA. The review will focus on models that were provided in the last 30 years. In the final part of the chapter, examples will be provided on using analytical models for estimating field plume lengths. The modeling exercises are aimed at examining the applicability of analytical models in *safely* predicting plume lengths.

2.2 Tabulating and Analyzing KORA Data

This chapter focuses on KORA projects that were associated with sites contaminated with organic contaminants. KORA data were obtained, generally, from employing advanced and the latest state of art measurement techniques. As such, higher reliability can be placed on these data. Naturally occurring physical as well as bio-chemical properties of the subsurface are dependent upon local hydrogeological events, such as seasonal variation, rain and flood events. In that sense, the data compiled in this thesis should be more helpful for similar further research in Germany than elsewhere. For tabulating data, the following three KORA thematic reports, out of eight, have been used: KORA thematic group 1 (see, *KORA TV-1*, 2008) that deals with petroleum hydrocarbons, KORA thematic group 2 (see, *KORA TV-2*, 2008) that deals primarily with coal tar oil and KORA thematic group three (see, *KORA TV-3*, 2008) that deals with chlorinated solvents. In this section the details on collecting and grouping data is provided first. Data analyses that is, primarily, centered on plume lengths are provided subsequently.

2.2.1 Grouping KORA data

In order to simplify analyses, data from the three KORA thematic groups are re-grouped into two contaminant groups, namely: Hydrocarbon Group (or HC, a group for Light Non-Aqueous Phase Liquids (NAPL)) and Chlorinated solvent group (or CS, a group for Dense Non-Aqueous Phase Liquids (DNAPL)). The HC group is further categorized into three different subgroups, namely: BTEX group, PAH group and Other Hydrocarbons (OH) group. The OH group comprises of compounds that are neither BTEX nor PAH nor CS. The tables in Appendix 1 provide the compiled data from KORA projects on HC and CS, respectively. Data have been collected of the parameters that are usually required for the analytical modeling purposes. The HC data table provides data of thirty-nine plumes, either BTEX, PAH or OH, originating from eight different sites from different parts of Germany. Data from laboratory or from models were only tabulated when field (measured) data were not available. No modification of the source data were done in compiling them. Some interpolating errors are possible for data that were originally provided in graphical form. In the next sub-sections statistical analyses of the compiled data are provided.

2.2.2 The Maximum Plume Length, L_{max}

For practical purposes, L_{max} is the distance between the origin of the contaminant source and the threshold concentrations, e.g., Maximum Contaminant Level

(MCL) provided by the regulating agencies, encountered downgradient of the source. A reference to an absolute zero concentration or a steady-state concentration downgradient of the source can also be used for defining L_{max}. The L_{max} tabulated for this chapter are based on the definitions provided by the authors of the KORA reports. Provided that data are reliable, a good approximate of L_{max} can be obtained from the descriptive statistics of field plume lengths and other field parameters. Figure 2.1 provides one such descriptive statistics of L_{max} for different groups of contaminants observed at KORA sites and tabulated in Appendix 1. In plotting Figure 2.1, the maximum value were used when the original data were provided in a range, whereas, specified values were used when the original data contained any of the inequality symbols. The median plume length of BTEX (= 135 m) in Figure 2.1 is shorter than the median value provided for non-service station BTEX sites (also all of the KORA BTEX sites) in other database studies, e.g., *Wiedemeier et al.* (1999), *Newell et al.* (1990). For service-station BTEX sites *Rice et al.* (1995) and *Newell et al.* (1990) report a significantly shorter median plume length than that is observed in Figure 2.1. *Teutsch et al.* (1997), who collected data of 76 sites from literature, provided slightly bigger median plume length for BTEX sites compared to that obtained from KORA sites. The median value (= 80 m) of OH plume lengths is comparable to BTEX plume lengths. The only site where Methyl-Tert-Butyl-Ether (MTBE) was a primary contaminant, produced a plume length of 2000 m (not used in the Figure 2.1, data provided in Appendix 1). MTBE together with heterocyclic aromatic compounds are among the contaminants that are recalcitrant to biodegradation.

The biodegradation of PAH compounds is dependent on the number of rings it possesses in its chemical structure. PAH compounds with more than 3 aromatic rings are found to be highly sorptive, whereas, PAH's with up to 3 aromatic rings are more mobile and less biodegradable. In general longer plume lengths, compared to BTEX, have been reported for PAH with 3 rings (*Teutsch et al.*, 1997). The median plume length for varying PAH compounds from different KORA sites is found to be 300 m, which is comparable to values for 2 and 3 ringed PAH's sites provided in *Teutsch et al.* (1997). Significantly longer plume lengths as compared to Hydrocarbons, often at least an order of magnitude longer, are observed in sites contaminated with Chlorinated Solvents (CS). The median plume length (= 2000 m) obtained from KORA sites is at least five times longer than the values provided in *Newell et al.* (1990) and in *Wiedemeier et al.* (1999), whereas, at least two times shorter value is provided in *Teutsch et al.* (1997). One of the several reasons behind the longer plume lengths is due to the presence of halogen (Chlorine) in their chemical structure. Dehalogenation, which normally requires anaerobic condition as well as a presence of an electron donor, is a pre-requirement for bio-degradation of CS (*Wiedemeier et al.*, 1999). When pre-requirements for bio-degradation are met, the plume lengths from CS can be significantly shorter

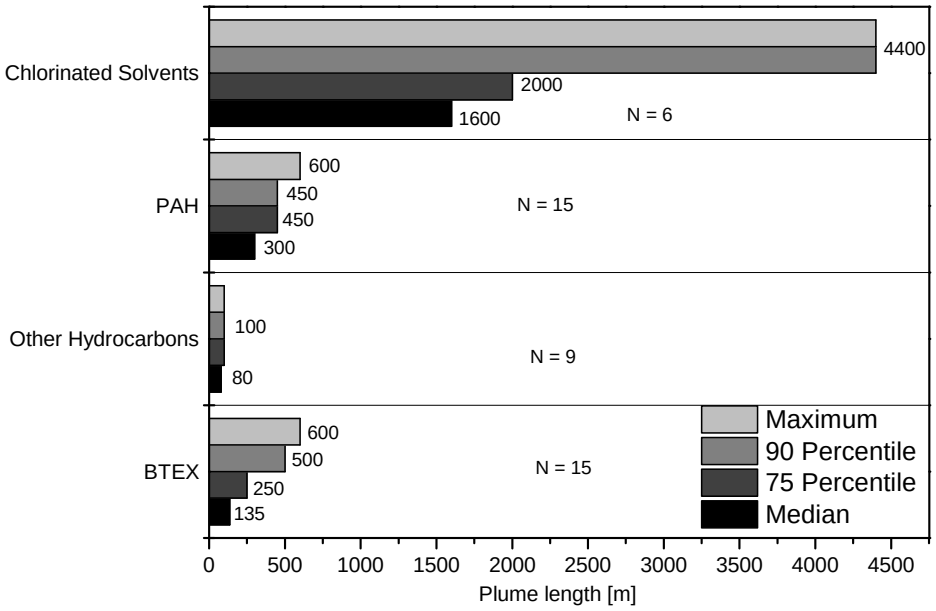

Figure 2.1: Plume lengths of different compound groups

than observed at KORA sites. *Wiedemeier et al.* (1999) also suggest that the results observed at KORA sites are likely when pre-condition for dehalogenation of CS are not met. It is important to consider the fact that the median values provided above were obtained from a comparatively smaller data set, only 6 data for CS for an example. Hence, precautions are recommended before using the results from this research.

2.2.3 Plume length and the other active parameters of NA

Mathematical analysis of the plume length provide it as a combined function of several aquifer and bio-chemical parameters. These are discussed, in detail, in the next sections. In this section, a simple linear correlation analysis is performed to check whether or not L_{max} relates to any of the single parameter that is considered to play significant role during NA.

As can be observed from Figure 2.2 and 2.3, BTEX plume lengths are found to be only slightly ($R^2 < 0.6$) correlating in the two cases: with aquifer conductivities (K) and with donor concentrations (ED). Conductivities are also marginally correlated to PAH plume lengths. Additionally, no correlation between L_{max} and aquifer thickness was found to exist for any of the compound groups. Due to lack of sufficient and explicit data, correlation analyses were not performed between different Electron Acceptors (EA) and plume lengths (see, Appendix 1). Furthermore, extreme data, for example the concentrations of MTBE or BTEX at the

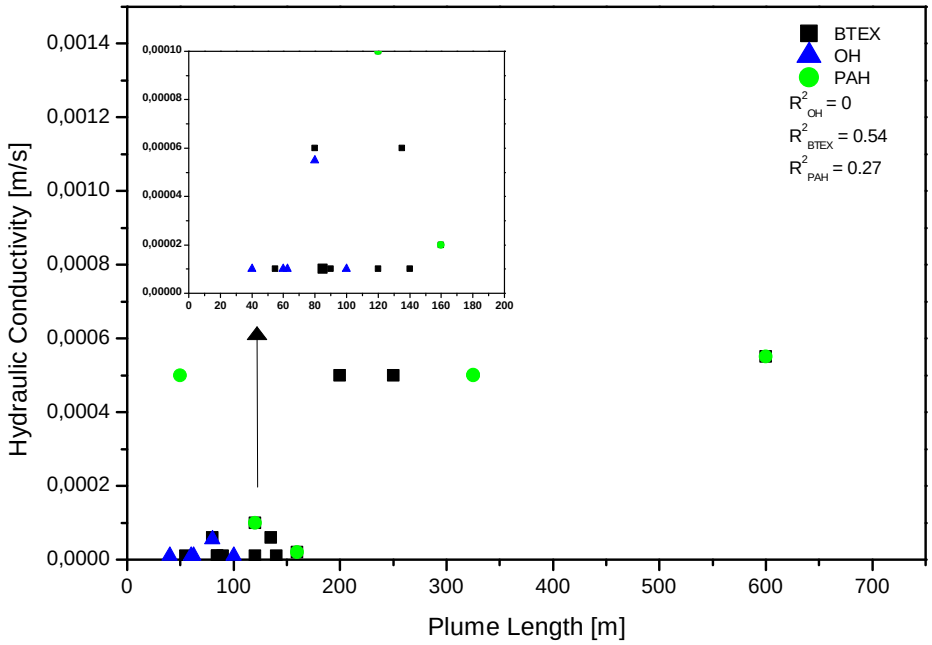

Figure 2.2: The maximum plume length and aquifer conductivity

Metlen site which are 290 mg/L and 230 mg/L (see, Appendix 1, 75^{th} percentile of BTEX = 10.5 mg/L and that of OH group = 8.5 mg/L), respectively, and few other such extreme data, were excluded from the correlation analysis. These exclusions were required as these few extreme data significantly distorted the analysis. Additionally, correlation analysis of chlorinated solvent data were not performed due to very few (only six) available data.

Wiedemeier et al. (1999), who meticulously gathered and analyzed data from several Air Force sites (mostly BTEX sites) in US, found plume length marginally correlating ($R^2 = 0.54$) with seepage velocity (v), which is a product of conductivity and the head gradient of the aquifer. The same authors also found a good correlation ($R^2 = 0.86$) between L_{max} and plume width. However, the provided discussion did not clarify if the selected plume widths were also the maximum plume width. Further, *Wiedemeier et al.* (1999) also found L_{max} not correlating with Electron Donor. This is opposed to the result obtained from the KORA data analysis (see Figure 2.3). Similar correlation analysis were performed by *Rice et al.* (1995), who analyzed over 1200 BTEX sites in US. *Rice et al.* (1995) found plume lengths not to correlate to any of the parameters mentioned above. Large scale statistical analysis of PAH plume data are not known to the authors. Quite clearly, the correlation analyses suggest that L_{max} must be a function of more than a single parameter observed in the aquifer.

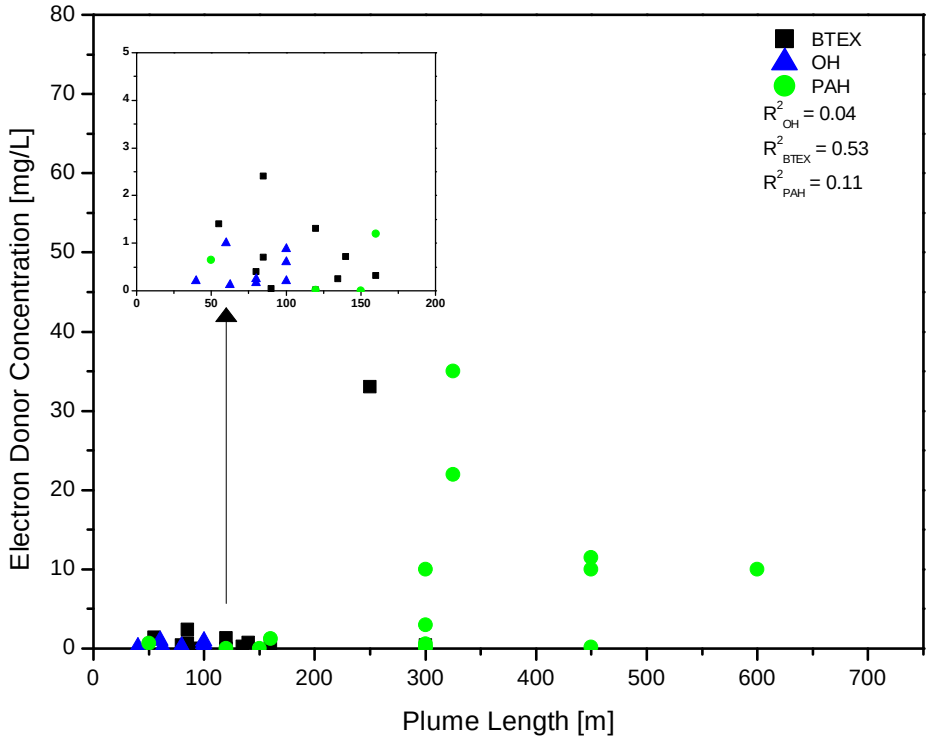

Figure 2.3: The maximum plume length and ED concentration

2.3 Analytical Modeling for Contaminated Site Assessment

Analytical models have a long development history (*Wexler*, 1992). From the very beginning their development have largely been based on the quantitative analysis of heat transfer in solid media. This section will focus on analytical models of reactive solutes that were developed after the 80's of the last century. In fact, it was only after 80's that the analytical models were more commonly used for site assessment purposes. A brief description of governing equations for solute transport in porous media is provided first. Subsequently, a review on development of analytical models and analytical models found in literature are provided.

2.3.1 Basic Concepts on Analytical Model Development

The fundamental equation that governs the transport of solute in porous media, called the Advective-Dispersive-Reactive (ADR) equation, has the following form

in vector notation:

$$\frac{\partial(\phi_e C)}{\partial t} = -\nabla \cdot [\phi_e v C - \phi_e D \cdot \nabla C] + \phi_e Q_s \tag{2.1}$$

In which, the first term on the right within the square bracket is the advective term, the second term is called the dispersive term and the last term, outside of the square bracket, is the source or sink term. The first two terms represent the physical processes (advection and dispersion) that results in change in concentration, C (M/L^3), with respect to position within the representative volume or domain. The third term, represented by Q_s $[M/L^3T]$ can include several combinations of physical, chemical or biological reactions that a solute undergoes or it can include non-reactive terms such as intrusion/extrusion of solute to/from the domain due to pumping, precipitation etc. Considering a uniform and constant average linear velocity (v $[L/T]$) aligned with the x-axis and additionally, if coefficients of hydrodynamic dispersion ($D = \alpha * v$ $[L^2/T]$, where α $[L]$, is a proportionality tensor called dispersivity) and effective porosity (ϕ_e $[-]$) are also held constant, then the 3D-ADR equation takes the following form in differential notation:

$$\frac{\partial C}{\partial t} = D_x \frac{\partial^2 C}{\partial x^2} + D_y \frac{\partial^2 C}{\partial y^2} + D_z \frac{\partial^2 C}{\partial z^2} - v \frac{\partial C}{\partial x} + Q_s \tag{2.2}$$

Where, x, y, z $[L]$ are the 3-axes of Cartesian co-ordinates and t $[T]$ is the selected time after which the change in C is to be quantified. Eq. (2.2) can be shortened to represent a 2D case, an infinitely deep or wide aquifer, or a 1D case, an infinitely deep and wide aquifer, by removing term(s) with D_y and/or D_z.

For modeling reactive transport, ADR equations are required to be solved for each solute (i.e., C is replaced by ED, EA and Product for the two-reactant system) participating in the reaction. Furthermore, an appropriate expression for Q_s is required to be added to each ADR equation before attempting a solution. The solution is required to be unique and constrained by the initial conditions and the boundary conditions (not discussed here, they can be found in standard textbooks, e.g., *Wiedemeier et al.*, 1999), both of which have to be explicitly specified for each participating solute. Analytical models, known so far, have all resulted from solving a linear form of ADR equations. This literally means that the selected expression for Q_s depends linearly on concentration. This restrictive selection leads to limitation on the applicability of analytical models. Next, some of the most common expressions for Q_s that have been used in developing analytical models are very briefly explained.

2.3.1.1 Common Source or Sink Expressions

Linear Sorption

Sorption, adsorption or absorption, of solute to aquifer media is one of the most common mechanisms that leads to removal of solute from groundwater. Mathematically, the removal of solute (ED) due to sorption is provided as:

$$Q_s = -\frac{\rho_b}{\phi}\frac{\partial S}{\partial t} \tag{2.3}$$

Where, ρ_b $[M/L^3]$ is a bulk density of solid matrix, ϕ $[-]$ is the total porosity, and S $[-]$ refers to mass of solute sorbed on solid matrix per unit mass of solid matrix. The negative sign on the right side of eq. (2.3) refers to loss of solute from groundwater. If it can be assumed that the sorption process is faster than the groundwater flow and that the sorption of solute is only the function of solute concentration in groundwater, then eq. (2.3) can be modified as:

$$Q_s = -\frac{\rho_b}{\phi}\frac{\partial S}{\partial ED}\frac{\partial ED}{\partial t} \tag{2.4}$$

for which the value for S is obtained from so called isotherm experiments. The linear isotherm model, among the several available in literature, is very commonly used for modeling reaction transport. The linear isotherm model provides S as:

$$S = K_d\, ED \tag{2.5}$$

where K_d $[L^3/M]$ is the linear partitioning coefficient. For modeling Non-Aqueous Phase Liquid (NAPL), contaminants or ED considered in this chapter, K_d is found to be uniquely related to the mass fraction (f_{oc}) of organic carbon in the porous medium. The relation is provided as:

$$K_d = K_{oc}\, f_{oc} \tag{2.6}$$

Where, K_{oc} $[L^3/M]$ is an organic carbon (in porous media) normalized partitioning coefficient. K_{oc} is compound specific and is found to correlate with octanol-water partitioning coefficient K_{ow} $[-]$. *Lyman et al.* (1982) provides the following empirical expression that relates K_{oc} and K_{ow}:

$$\log K_{oc} = A\, K_{ow} + B \tag{2.7}$$

Where, A and B are empirical coefficients, which depends on the composition of the organic matter and on the experimental conditions. *Lyman et al.* (1982) provides A=0.937 and B=0.006, when K_{oc} is expressed in cm^3g^{-1}.

First-Order Chemical Reaction

At sites contaminated with organic contaminants, redox reaction between Electron Donor (ED, contaminant) and Electron Acceptor (EA, partner reactant, e.g., O_2, NO_3) can be the most dominant form of reaction. It is also very likely that reactions are slow and they are required to be treated kinetically. Much simpler are those reactions for which equilibrium can be reached rapidly. In such case, the Q_s is generally replaced with the reaction kinetics expression, which is provided for two reacting solutes resulting to irreversible product, i.e., ED + EA $\longrightarrow$ Product as:

$$Q_s = \frac{dED}{dt} = -\phi k EA \cdot ED \tag{2.8}$$

where k $[L^3/MT]$ is the second order reaction rate coefficient. Eq. (2.8) is simplified by assuming an abundance of EA in comparison to ED in groundwater, which is often encountered at sites. This converts eq. (2.8), a second-order kinetic model, to a pseudo first-order kinetic model as:

$$Q_s = \frac{dED}{dt} = -\phi \lambda \cdot ED \tag{2.9}$$

where $\lambda = k \cdot EA$ $[T^{-1}]$, in which k refers to rate of loss of EA from the groundwater. The right hand side of eq. (2.9) replaces Q_s in eq. (2.2) when analytical model for solute transport with first-order reactions rate is developed.

Instantaneous Reaction Model

The instantaneous reaction model, also called Elector-Acceptor or Electron-Donor limited model, considers that the reaction between the EA and ED is limited by their transport, i.e., the reaction rate is faster than the groundwater flow. This model was first proposed by *Borden and Bedient* (1986) and it has been mostly used in recently proposed analytical models. For a simple case, i.e., ED + EA $\longrightarrow$ Product, the change in ED concentration to the concentration is provided as:

$$Q_s = \Delta ED = -\frac{[EA]}{\gamma} \tag{2.10}$$

where ΔED $[M/L^3]$ refers to change in contaminant concentration due to reaction and γ $[-]$, which can be obtained from reaction stoichiometry, is called the

utilization factor. As no reaction kinetic data are required, instantaneous reaction model provides a very simple alternative to model reaction transport of solute in subsurface.

Monod Kinetics Model

If the role of the microorganisms are to be accounted in the model, then the Q_s term is required to include bio-reactions kinetic expression. The most common bio-reaction kinetics model is the one provided by *Monod* (1942), often also referred to as Michaelis-Menten kinetics. For the two reactants system the Monod model has the following form:

$$Q_s = -kX \frac{EA}{K_{EA} + EA} \frac{ED}{K_{ED} + ED} \tag{2.11}$$

in which, K_{EA} $[M/L^3]$, K_{ED} $[M/L^3]$, and k $[T^{-1}]$ are the half velocity constants for EA, ED, and maximum specific rate of substrate utilization, respectively. X $[M/L^3]$ is the microbial concentration. Eq. (2.11) is generally simplified to a so called single Monod model. This is achieved by assuming $K_{EA} >> EA$. Furthermore, in order to account for the growth of microorganisms as per loss of ED, a coefficient (y $[-]$), called yield coefficient, is introduced to the Monod model (eq. 2.11), which then takes the following form:

$$Q_s = r = -k \frac{X}{y} \frac{ED}{K_{ED} + ED} \tag{2.12}$$

In order to include the death or decay of the microorganisms, eq. (2.12) is accompanied by an expression of change of X as a function of time:

$$Q_s = -kXy \frac{ED}{K_{ED} + ED} - bX \tag{2.13}$$

where b $[T^{-1}]$ is the first order decay coefficient that accounts for the death of microorganisms. For steady-state, eq. (2.11) without the EA term and eq. (2.13) can be combined to obtain $Q = bX/y^2$, which can be used for Q_s term in ADR equation.

Any one, more than one, or all of the expressions provided above can be summed and added to the ADR equation for Q_s. In addition, expressions for volatilization, dilution etc., can also be included. In general, almost all of the analytical models in literature (described in next subsection) have considered only one or at most two of the above expressions. Analytical solution may not be possible

if the complexity of ADR equation is increased. Even if a solution can be found, the resulting model will require too many initial information and parameters for their application. Next, a brief review is made of analytical models provided in literature.

2.3.2 Analytical Models for predicting L_{max}

Before describing a particular model, it is important that an outline of the most important and common assumptions that are made in developing these models be stated. Analytical models, in general, are developed for two main purposes. First, for the verification of the numerical models and second, for the pre-assessment or rapid estimate of site parameters. As has been discussed earlier, analytical model simplifies the actual field condition, e.g., linearizing processes, in order to provide a simple solution of the field dynamics. Some of the very common simplifications that are made are: a homogeneous domain, uniform flow velocity, porous medium is fully saturated, dispersion and diffusion are constant and compound-independent, and selection of linear expression for the source or sink term. These simplification definitely hinders the applicability of the analytical models. However, on a positive side, these (assumptions) may lead to overestimation, which is desired for a contaminated site scenario, of parameters to be quantified (see section 2.4). In the following some of the most important and recent analytical models that can be used for contaminated sites assessment is provided. The described models are all at least 2D analytical models and all of them have included at least one of the source or sink expression discussed above.

The Domenico Model

The Domenico Model is based on the approximate analytical solution of ADR equation with a first-order source/sink term (eq. (2.9)) provided in *Domenico* (1987). The solution is based on all assumptions that are stated above (in section 2.3.2). The contaminant source is independent of the aquifer geometry and has a finite width and finite thickness. The model combines the conservative solute transport solution of *Domenico and Robbins* (1985), provided as:

$$ED(x,y,z,t) = \frac{ED_0}{8}\,\mathrm{erfc}[(x-vt)/2\sqrt{(\alpha_x vt)}]\cdot \left\{\mathrm{erf}\,[(y+W/2)/2\sqrt{(\alpha_y x)}] - \mathrm{erf}\,[(y-W/2)/2\sqrt{(\alpha_y x)}]\right\}\cdot \left\{\mathrm{erf}\,[(z+M/2)/2\sqrt{(\alpha_z x)}] - \mathrm{erf}\,[(z-M/2)/2\sqrt{(\alpha_z x)}]\right\} \tag{2.14}$$

with the following one dimensional transport model with the first-order degradation provided by *Bear* (1979):

$$ED(x,t) = \frac{ED_0}{2} \exp\left\{x/2\alpha_x[1-\sqrt{1+4\lambda\alpha_x/v}]\right\} \cdot \\ \text{erfc}\left\{[x-vt\sqrt{1+4\lambda\alpha_x/v}]/2\sqrt{\alpha_x vt}\right\} \tag{2.15}$$

to provide an expression for an time dependent concentration isosurface as:

$$ED(x,y,z,t) = \frac{ED_0}{8} \text{ exp } \left\{x/2\alpha_x[1-\sqrt{1+4\lambda\alpha_x/v}]\right\} \cdot \\ \text{erfc}\left\{[x-vt\sqrt{1+4\lambda\alpha_x/v}]/2\sqrt{\alpha_x vt}\right\} \cdot \\ \left\{\text{erf }[(y+W/2)/2\sqrt{(\alpha_y x)}] - \text{ erf }[(y-W/2)/2\sqrt{(\alpha_y x)}]\right\} \cdot \\ \left\{\text{erf }[(z+M/2)/2\sqrt{(\alpha_z x)}] - \text{ erf }[(z-M/2)/2\sqrt{(\alpha_z x)}]\right\} \tag{2.16}$$

where ED_0 $[M/L^3]$ is the initial concentration and W and M $[L]$ are the width and the depth of the source, respectively. erf and erfc are error function and complementary error function, respectively. The steady-state plume length can be obtained from eq. (2.16) by setting the argument of erfc to negative two or smaller. At the steady-state, L_{max} can be obtained at the centerline of the plume, i.e., at $y = 0$ and $z = 0$, from:

$$ED(x) = ED_0 \text{ exp } \left\{x/2\alpha_x[1-\sqrt{1+4\lambda\alpha_x/v}]\right\} \cdot \\ \cdot \left\{\text{erf}[W/4\sqrt{\alpha_y x}]\right\} \left\{\text{erf}[M/4\sqrt{\alpha_z x}]\right\} \tag{2.17}$$

Several modifications were done to the Domenico model when it was implemented in a spreadsheet software, BIOSCREEN, by EPA (see *EPA*, 1996). Among the major modifications were changing the first-order decay model (eq. (2.9)) with an instantaneous decay model (eq. (2.10). Based on a superposition technique, the instantaneous model was adopted to include multi-EA and an ED reaction. In addition, the sorption (eq. (2.4)) model was also included. The original and modified Domenico model has been applied to several field sites, e.g., by *Wiedemeier et al.* (1999), *Newell et al.* (1995) and others.

Several authors have reported limitations of the Domenico model. *Guyonnet and Neville* (2004) have shown that the concentration profile resulting from the Domenico model is only accurate along the centerline of the plume and that inaccuracy increases with the increase of lateral distance from the centerline. Fortunately,

this limitation is not important if the goal is to obtain L_{max}. Another limitation, suggested by *Srinivasan et al.* (2007), relates to the dispersivity value that are input to the Domenico model. *Srinivasan et al.* (2007) suggest that the Domenico model will provide a better estimate when longitudinal dispersivity values are low, seepage velocities are high, and simulation times are large. Again, the suggested limitations may not hinder if the estimation of L_{max} or steady-state plume is to be made using the Domenico model. This is because, the longitudinal dispersivity has been shown to have only minimal impact on plume length in several of the recent studies, e.g, *Liedl et al.* (2005), *Ham et al.* (2004), and that several years to decades are required for the plume to reach a steady-state condition (e.g., case study in *Wiedemeier et al.*, 1999). More recent works, e.g., *Huang et al.* (2003) and others, have shown that the degradation of contaminant is concentrated along fringes of the plume; rather than along the longitudinal flow path as has been considered in the Domenico model. No study is known to have rigorously compared the results from Domenico model with the same obtained from the models that have considered fringe centered degradations.

The Ham et al. Model

The Ham et al. model is provided in *Ham et al.* (2004). The model solves the 2D ADR equation (eq. (2.2)) with inclusion of instantaneous model (eq. (2.10)) for the source/sink term. The aquifer in the model is considered infinitely thick but with a finite source width (W). The ED with concentration (ED_0) is continuously injected with the rate Q $[L^3/T]$ at the midpoint of the aquifer width, i.e., at $W = 0$. The EA with input concentration (ED_0) enters the domain from location beyond the injection point of ED along the width of the aquifer. For the model, the reaction between EA and ED is assumed to be concentrated at the edges of the plume. Further, for providing an explicit expression for L_{max} the model considers all assumptions provided in section 2.3.2. The slightly modified form of Ham et al. model at steady-state, required for L_{max} calculation, can be stated as:

$$L_{max} = \frac{1}{4\pi} \frac{\gamma E D_0^2 \, Q^2}{E A_0^2} \frac{1}{v^2 \, \alpha_y} \tag{2.18}$$

where γ $[-]$ refers to utilization factor defined in eq. (2.10) and α_y $[L]$ is transverse dispersivity in horizontal direction. The Ham et al. model clearly nullifies the role of longitudinal dispersivity (α_x) for the plume at steady-state, which was considered to play a significant role previously, for e.g., in the Domenico model. Another important aspect of the Ham et al. model is that the entire model can be grouped into two terms instead of several parameters. The first term, which includes all parameters that effect concentration and reaction of EA and ED, can

be called the **chemical term**. Similarly, the term that affects the position of the EA and ED in the domain, e.g., dispersion coefficients, flow velocity, can be grouped as the **mixing term**. Eq. (2.18) has been arranged according to these terms. This kind of grouping can be useful if parameter estimation techniques or uncertainty analysis are to be performed. Ham et al. model is not known to have been verified in the field setting or from lab experiments.

The Liedl et al. Model

The Liedl et al. model, referring to the model provided in *Liedl et al.* (2005), considers a vertical 2D domain with the continuous line contaminant source (ED, M $[L]$) that penetrates the entire thickness of the aquifer. The aquifer is considered infinitely wide, in contrast to the Ham et al. model in which aquifer was infinitely deep. The Liedl et al. model considers the fringe-centered degradation of ED based on the instantaneous model (eq. (2.10)), for which the supply of EA is from the top of the aquifer. Based on these set-up and all the assumptions provided in section 2.3.2, the Liedl et al. model provides the following explicit expression for quantifying L_{max}:

$$L_{max} = \frac{4}{\pi^2} \ln\left(\frac{4}{\pi}\frac{\gamma\, ED_0 + EA_0}{EA_0}\right)\frac{M^2}{\alpha_z} \tag{2.19}$$

where α_z $[L]$ is transverse dispersivity in vertical direction and subscript "0" in ED and EA refers to their concentrations at the source. Mathematically, the Liedl et al. model is very similar to the Ham et al. model discussed earlier. The Liedl et al. model verifies the conclusion on α_x that the Ham et al. model suggested. As was considered for the Ham et al. model, the L_{max} provided by the Liedl et al. model can also be considered as a simple product of the chemical term and the mixing term. If KORA data are to be used, then the chemical term for BTEX sites will have a value between 0.0053 and 89.125, with median value of 0.28. For this calculation, $\gamma = 3.14$ (provided in *Wiedemeier et al.*, 1999) and average background concentration of EA , i.e., for O_2= 8 mg/L, were considered. Likewise, the mixing term will have a value between 30 m and 10^5 m with the median value of 1445 m when $\alpha_z = 5$ cm is considered.

The key assumption, in the Liedl et al. model, on the ED at the source penetrating the entire aquifer thickness is likely to be never observed in the field. The data provided in *Wiedemeier et al.* (1999) show thats the penetration of BTEX in aquifers is not very much over a meter. Therefore, using thicker source, the L_{max} provided by the Liedl et al. model should definitely be an overestimate (see section 2.4 for examples) and hence safe. However, it remains to be clearly established how much of an overestimate can be considered a good estimate. *Grajales*

(2011) rigorously compared over seventy field L_{max} with those provided by the Liedl et al. model and concluded that for the $Z > 8$ m, $ED_0 < 1$ mg/L and $\alpha_z > 6$ cm, the model L_{max} will be at least two times longer than that of the field. *Bajracharya* (2011) and *Yadav et al.* (2012), using numerical techniques, showed that the model L_{max} will be longer by over ten times when the ED penetration in aquifer is less than twenty five percent of the aquifer depth. *Maier and Grathwohl* (2006), who performed over hundreds of simulations of scenarios matching the Liedl et al. model scenario, provided the following empirical expression for L_{max}:

$$L_{max} = a \left(\frac{\gamma\, ED_0}{EA_0} \right)^b \frac{M^2}{\alpha_z} \tag{2.20}$$

with $a \approx 0.5$ and $b \approx 0.3$. The Liedl et al. model can easily be equated with the empirical expression provided by *Maier and Grathwohl* (2006). Very recently, Liedl et al. model has been extended to cover a planar source in a 3D domain in *Liedl et al.* (2011) (for detail see chapter 3).

The Chu et al. Model

The Chu et al model, provided in *Chu et al.* (2005), solves the 2D-ADR equation (eq. (2.2)) with inclusion of Monod kinetics model (eq. (2.8)) and the instantaneous model (eq. (2.2)) for the steady-state condition. The reaction between EA and ED is assumed to be centered at the fringe of the plume. The aquifer in the Chu et al. model is infinitely deep, similar to Ham et al. model, and the finite line source (W) is horizontally oriented perpendicular to the direction of flow. Further, assumptions that the Chu et al. model uses are provided in section 2.3.2. The slightly modified resulting explicit expression for the L_{max} provided in *Chu et al.* (2005) is

$$L_{max} = \frac{\pi}{16} \left[\frac{\gamma\, ED_0}{EA_0 - \epsilon} \right]^2 \frac{W^2}{\alpha_y} \tag{2.21}$$

where ϵ $[M/L^3]$ is the parameter that is only related to the Monod Kinetics parameters- K_{EA} and K_{ED} (see eq. (2.9)). *Chu et al.* (2005) suggest that $\epsilon << K_{EA} + K_{ED}$. The two models, Chu et al. and Liedl et al., define L_{max} as directly proportional to the square of source geometry (W or M) and inversely proportional to the transverse mixing. This translates to the higher importance of quantifying the source dimensions if these analytical models are to be used for the site assessment purpose. The Chu et al. model is not known to have been used in laboratory or the field setting, except a field example provided in *Chu et al.* (2005) in which an extremely large and impractical L_{max} was obtained.

Other Models

Apart from the models described above, few other similar models can be found in literature that can be used for the analysis of the contaminant plumes. *Gutierrez-Neri et al.* (2009) combined the Domenico model, a plume centered-degradation, with the fringe-centered degradation model in a recent work. The combined model provided an explicit expression for L_{max} as:

$$L_{max} = \frac{MW}{4\pi\sqrt{\alpha_y\alpha_z}(EA_0/\gamma ED_0 + EA_0) + MW\lambda/v} \tag{2.22}$$

Gutierrez-Neri et al. (2009) used a field site to explain the applicability of the combined model, however, the approach used in developing the model was critically received by *Hunkeler et al.* (2010).

Semi-analytical models that provide distribution of EA, ED and the biomass in the 2D domain have been proposed in *Cirpka and Valocchi* (2007) and *Cirpka* (2010). The Chu et al. model is more rigorously treated in *Cirpka and Valocchi* (2007) and in addition, a closed-form solution is provided of the ADR equation that includes the Monod model (eq. 2.8) with bacterial growth limited by the reactant concentration as a source/sink term. *Cirpka* (2010) further simplifies the process from which the distribution of EA, EA and the biomass in the domain can be quantified. The *Cirpka and Valocchi* (2007) models were used to simulate the microcosm results of *Bauer et al.* (2009).

The analytical models discussed above clearly provide a wide variety of choices to fit to many field scenarios. With very few data requirements, these analytical models can definitely be a tool of choice for the pre-assessment of contaminated sites. However, a tricky question that remains to be answered is, "which models to select for a particular field site?" As an initiative step, a spreadsheet software, which can aid in selection of the best model for a particular site, was developed in *Yadav et al.* (2011).

2.4 Examples on Using Analytical Models for Site Assessment

Several analytical models were discussed in the previous section. In this section few modeling exercises will be performed to evaluate their applicabilities. The modeling exercises are more rigorously tackled in *Grajales* (2011). For the example exercises two different analytical models, the 2D Liedl et al. model and the BIOSCREEN model that is based on the Domenico model, are used. The Liedl

Table 2.1: Field data used in analytical modeling.

Site/ (Compound)	Aquifer Thickness (m)	Plume length (m)	ED (mg /L)
Niedergrsdorf TL1 (m/p-Xylol	5-12	120	1.3
OLES Epple (DRM: BTEX)	5-15	160	0.31
VMZ Spandau 1.GWL (BTEX)	11	250	33
Castrop-Rauxel 1.Stockwerk (Benzol)	5-7.4	200	123
Metlen (BTEX)	1.5-6	500	230

et al. model is a fringe-centered degradation model in which the EA enters the domain from the top, whereas, the BIOSCREEN models is a plume core-centered degradation model in which the EA and ED mix along the flow path. The selected sites, for modeling, are marked with "$*$" in the table provided in Appendix 1. The site selection was primarily based on the availability and reliability of the site's data and information (e.g., steady-state condition). The fact that BIOSCREEN has been previously used mostly to simulate BTEX sites was also a point considered in selecting sites. Also considered were the contamination scenarios, i.e., fuel storage sites or industrial site, and the geographic locations (i.e., different subsurface properties) of the sites. *KORA TV-1* (2008) provides a very extensive details of the selected sites. The major obstacle for the modeling exercises is the non-availability of certain critical parameters, more specifically the values of different dispersivities (α_x, α_y and α_z) and the source dimensions. Dispersivities cannot be directly measured and therefore, they are obtained from the model calibration routine, which often requires more site data as well as longer time. An alternative approach could be to estimate dispersivity value that in several cases provide safer predictions if not very accurate predictions of the L_{max}. Hence, an additional objective of the modeling exercises was to find an appropriate estimate of unknown critical parameters.

As dispersivity values were mostly not available from the KORA reports (therefore not tabulated, see appendix 1), approximations were made to find a single dispersivity value that provided the best estimate or the safe estimate of the plume length for most of the modeled sites. After several trials, it was found that the $\alpha_z = 5$ cm provided the best results for both compared models. Based on the information provided in the manual of the BIOSCREEN model, $\alpha_y = 10 * \alpha_z$ and $\alpha_x = 20 * \alpha_y$ were set. Additionally, the source width W required by the BIOSCREEN model was set to five times the depth of the aquifer. The source thickness for the BIOSCREEN was made very large (100$*$aquifer depth, several simulations were before fixing this thickness). This essentially converts the 3D BIOSCREEN model to behave as a 2D model (see, eq. 2.14 in which the large M

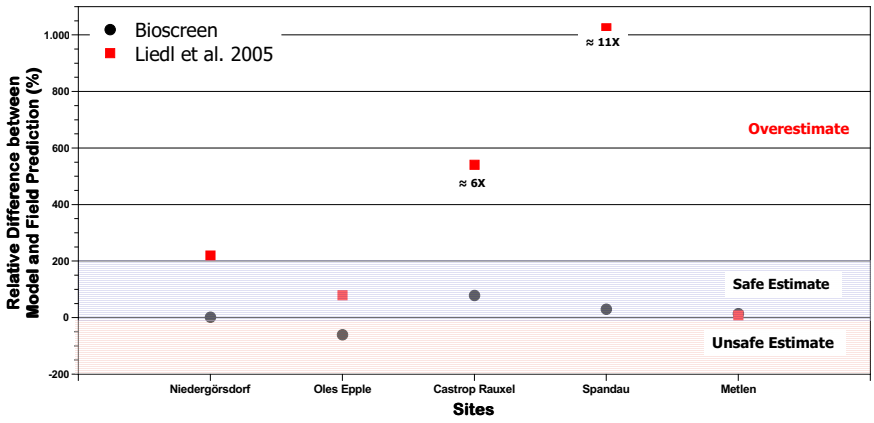

Figure 2.4: Comparing L_{max} from field and ones provided by BIOSCREEN model and the 2D-Liedl et al. model. For the model EA = 8 mg/L and α_{Tv} = 5 cm. Other data used in the model is provided in Table A.1

makes the erf term with M equal to unity). Thus, for the modeling exercises the two 2D models were compared.

In Figure 2.4 the results from the modeling exercises are provided. The L_{max} for the modeling exercise was defined as the distance from the origin of the source to the point where no contaminant was observed along the groundwater flow direction. The 0 % error in the vertical axis refers to the point at which the field plume length is equivalent to the model plume length, i.e, the exact prediction. Hence, any point below the 0 % point is an unsafe prediction or underestimation. Likewise, any point above the 0 % is both safe and an overestimate prediction.

Figure 2.4 clearly show that BIOSCREEN model estimates are relatively more accurate compared to the Liedl et al. model. On the other hand, the Liedl et al. model is found to overestimate almost in all of the tested cases, thus providing *safer* estimates. The safer margin at 200 % portrayed in the Figure 2.4 is rather qualitative, as distinguishing between a safer estimate and the overestimate is beyond the scope of this modeling exercises. As source thickness in the Liedl et al. model equals to the aquifer thickness, an extremely unlikely case for BTEX, the overestimated L_{max} were rather expected. Although overestimate is safe, the cases with very large $\sim$ 11X and $\sim$ 6X in the Figure 2.4 requires appropriate explanations. From KORA data (appendix 1) it is found out that these overly large plume lengths are obtained when both the source thickness and the contaminant concentration are very much above the average values. The BIOSCREEN model resulted in one unsafe prediction and that was observed at the site where the concentration of electron acceptors (NO_3 and SO_4) were significantly higher than

the average observed at all KORA sites.

In general, both models seem to provide good predictions of the L_{max} for the sites for which the model parameters have values that are generally observed at contaminated sites. Despite limitations of the Domenico model (or the BIOSCREEN model) discussed in section 2.3.2, it is found to provide a good estimate for most of the cases. On the other hand, although the Liedl et al. model always provided a safe estimate of L_{max}, the two out of five results can be considered significant overestimates. These all points to uncertainties in using analytical models for site assessment. More rigorous modeling exercises are required before these models can be brought to practical use.

2.5 Conclusions

In this chapter the KORA sites data, which are generally required for the analytical modeling of Natural Attenuation, were compiled and analyzed. Data analyses were primarily focused on the steady-state or the maximum plume lengths (L_{max}). The data analyses provided comparable (average for BTEX = 135 m and PAH = 300 m) results for Hydrocarbon Contaminated sites to those found in the literature (e.g., *Teutsch et al.*, 1997, *Rice et al.*, 1995 and others). Correlation analysis of the plume lengths from KORA data with other active field parameters suggested that the plume length is more likely to be a function of groups of several hydrogeological and bio-geo-chemical parameters than related to any single parameter. This result agrees with the analytical models, which are briefly reviewed for a major part of this chapter, that focuses on quantifying L_{max} and analyzing contaminant plume. From the literature review it was realized that there exist many analytical models, encompassing several field scenarios, that can be used for the site assessment purposes. The review of the analytical model also showed that L_{max} is likely to higher dependence on source geometry and transverse dispersivities than any other field parameters. In the last part of the chapter, modeling works were performed to compare L_{max} from field and that provided by the BIOSCREEN model and the Liedl et al. model. Results of modeling of five different BTEX KORA sites showed that these models can provide safe estimates (cases with overestimate rather than underestimate) of L_{max} for the site with average conditions. Modeling results also proved that α_z= 5 cm and $\alpha_y = 10 * \alpha_x$ as very safe estimates for these parameters in predicting plume lengths.

Chapter 3

A 3D analytical solution providing maximum plume length for a fully penetrating and finite width contaminant source

3.1 Introduction

[2] Contamination of aquifers with organic pollutants resulting from accidental spills or from inadequate handling of their storage facilities is common (e.g., *Teutsch et al.*, 1997; *Wiedemeier et al.*, 1999). Despite several large-scale contaminated site management related projects, like the very recently completed KORA project in Germany (http://www.natural-attenuation.de), the processes controlling and limiting contaminant spread have not yet been fully understood. Lack of adequate description and interpretation of small-scale subsurface heterogeneities, which affect transport and mixing parameters such as conductivity, dispersivity, pose a major challenge in appropriately assessing a contaminated site (*Bauer et al.*, 2009; *Cirpka et al.*, 1999; *Grathwohl et al.*, 2001; *Werth et al.*, 2006).

Based on numerous research activities conducted in the last two decades, where an electron donor (ED, e.g., petroleum hydrocarbons) resides in an aquifer with soluble electron acceptor (EA, e.g., oxygen), the following conclusions on contaminant spread in subsurface are generally accepted: 1) The steady state extension

[2]Part of the chapter is published as: Liedl, R., P. K. Yadav, and P. Dietrich, (2011), Length of 3D mixing-controlled plumes for a fully penetrating contaminant source with finite width, *Water Resour. Res., 47*, W08602, doi: 10.1029/2010WR009710.

of plumes range from less than a hundred meters to over a kilometer, depending on the type of contaminant (*Grathwohl et al.*, 2001; *Teutsch et al.*, 1997; *U.S. National Research Council*, 2000; *Wiedemeier et al.*, 1999). 2) The degradation of contaminants is in many cases focused to the plume fringes, where also the microbial population is concentrated (*Huang et al.*, 2003; *Thullner et al.*, 2002). 3) The mixing of mobile reactants that result in contaminant degradation is mostly controlled by transverse dispersivities, which can also be considered as the most critical parameter for a successful contaminated site assessment (*Cirpka*, 2002; *Grathwohl et al.*, 2001). Longitudinal dispersivity, on the other hand, has no or only minimal impact on overall contaminant degradation (*Ham et al.*, 2004; *Huang et al.*, 2003; *Liedl et al.*, 2005). 4) The instantaneous reaction model can be used to model microbially mediated biodegradation of the ED for the cases where the reaction is limited by the transport of reactants (ED or EA) (*Chu et al.*, 2005; *Koussis et al.*, 2003). However, for contaminants that have slower degradation rates or when transport rates of reactants in the aquifer are very high, kinetic models may have to be used (*Wiedemeier et al.*, 1999).

The incorporation of chemical and biological processes to the already complex groundwater flow system makes contaminated site assessment very difficult to interpret appropriately, although significant advances have been made (e.g., *Prommer et al.*, 2002). The extension of a plume and the concentration values near its downstream end become the decisive factors when concerns are focused on off site plume discharges from contaminated sites or where discharge may occur to ecosystems. In the past two decades, several attempts have been undertaken to derive explicit expressions for the extension of contaminant plumes by solving the advection-dispersion equation with or without degradation. The early works of *Domenico and Robbins* (1985) and *Domenico* (1987) provided a framework for multi-facet analysis of contaminant plumes and determination of plume parameters from the concentration profile. Further, the works of *Bekins et al.* (1998), *McNab and Dooher* (1998) and *Martian et al.* (2003) improved estimations of the biodegradation rates to be used in modeling microbial action in assessing contaminant spread. *Olsson et al.* (2004) and *Cirpka et al.* (2005) specifically investigated the dispersion term that is contained in the solutions of *Domenico and Robbins* (1985) and *Domenico* (1987).

The analytical models provided by *Domenico and Robbins* (1985) and *Domenico* (1987) considered biodegradation in the core of the plume. The works of *Thullner et al.* (2002), *Huang et al.* (2003) and others have clearly demonstrated that biodegradation reaction are (specially in the petroleum hydrocarbon contaminated sites) often concentrated at the fringe of the plume. This scenario is covered by, e.g., *Ham et al.* (2004), *Chu et al.* (2005), *Cirpka et al.* (2005), *Liedl et al.* (2005) and others (all 2D models). Interestingly, all of these fringe degradation models provide a formula for calculating plume length that is a function of source di-

mension (except *Ham et al.* (2004), who used point source), dispersivity, and the concentration ratio of the reactants. A major difference between them is related to source geometry and its orientation, that is, point source (e.g., *Ham et al.*, 2004)) versus line source (e.g., *Cirpka et al.*, 2005) and horizontally oriented source (e.g., *Chu et al.*, 2005) versus vertically oriented source (e.g., *Liedl et al.*, 2005). Numerical modeling approaches have also been employed to obtain a simple formula to calculate plume length. An empirical formula employing numerical approaches provided by *Maier and Grathwohl* (2006) is, specially, noteworthy here due to its striking similarity with the analytical formulas provided by the above-mentioned fringe degradation models. Further studies have focused on inclusion of subsurface heterogeneities in the mathematical description of reactive processes (e.g., *Werth et al.*, 2006) and in combining core and fringe degradation models (e.g., *Gutierrez-Neri et al.*, 2009). Quite recently, the combined model of *Gutierrez-Neri et al.* (2009) has been critically received by *Hunkeler et al.* (2010).

In this chapter a 3D contaminant plume scenario is considered involving a two species reaction. An implicit formula for the plume length is derived and analyzed based on the earlier work of *Liedl et al.* (2005). To obtain the plume length from the implicit expression, a simple numerical solution is provided and is implemented in an Excel^{TM} spreadsheet. The 3D and the 2D model of *Liedl et al.* (2005) are compared based on the plume lengths obtained for different mixing and source geometries. The impact of source shape on plume length is investigated and, finally, sensitivity analyses are performed to qualitatively rank parameters of the 3D model according to their influence on the plume length.

3.2 Theoretical Model Development

3.2.1 Model Setup

The model scenario is portrayed in Figure 3.1. A steady state plume of contaminant ("electron donor" or ED) is assumed to have developed in a shallow homogeneous aquifer. An ED and an Electron Acceptor (or EA, the reactant partner for ED) are assumed to be separated by the sharp front along the plume fringes, where an instantaneous reaction takes place. The symmetric 3-D model domain is infinite in y in both directions, extends from zero to positive infinity in x-direction and from $z = 0$ at the aquifer top to the plane $z = M$ representing an impervious aquifer bottom. The contaminant source is located at $x = 0$, has a finite width from $-W$ to $+W$ along the y-direction and extends over the entire aquifer depth (i.e., from $z = 0$ to $z = M$). This model set-up is expected to be of practical importance for shallow aquifers and for aquifers with large hydraulic head fluctuations (*Wiedemeier et al.*, 1999). For deeper aquifers the assumed model set-up

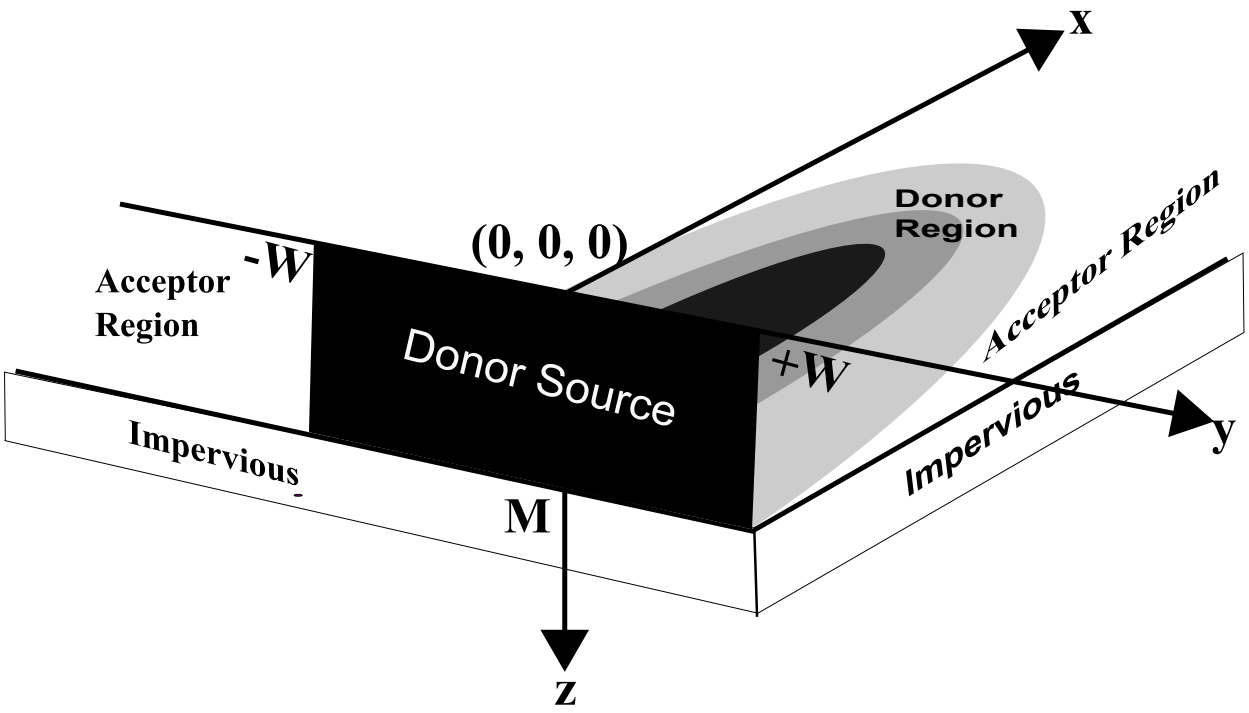

Figure 3.1: The basic model setup.

should provide conservative estimates of plume extension.

For the modeling approach, apart from a shallow homogeneous aquifer and a binary type instantaneous reaction between EA and ED concentrated at the fringe of the plume, a uniformly distributed concentration of the ED and a uniform flow field parallel to the x-axis are assumed. Accordingly, if dispersion is represented by the standard approach, i.e., a linear function of velocity, the transport equations for the ED and the EA in the steady state can be written as:

For ED:

$$v\frac{\partial C_D}{\partial x} - (\alpha_L v + D_D)\frac{\partial^2 C_D}{\partial x^2} - (\alpha_{Th} v + D_D)\frac{\partial^2 C_D}{\partial y^2} - (\alpha_{Tv} v + D_D)\frac{\partial^2 C_D}{\partial z^2} = -r \quad (3.1)$$

with the following boundary conditions:

$$C_D(0, y, z) = \begin{cases} C_D^\circ & \text{if } -W \leq y \leq +W \\ 0 & \text{else} \end{cases}$$

$$C_D(x, y, z) = 0 \text{ in “acceptor region”}$$

$$\frac{\partial C_D}{\partial z}(x, y, M) = 0 \text{ in "donor region" (no flux condition)}$$

Likewise for EA:

$$v\frac{\partial C_A}{\partial x} - (\alpha_L v + D_A)\frac{\partial^2 C_A}{\partial x^2} - (\alpha_{Th} v + D_A)\frac{\partial^2 C_A}{\partial y^2} - (\alpha_{Tv} v + D_A)\frac{\partial^2 C_A}{\partial z^2} = -\gamma r \quad (3.2)$$

with the following boundary conditions:

$$C_A(0, y, z) = \begin{cases} 0 & \text{if } -W \leq y \leq +W \\ C_A^\circ & \text{else} \end{cases}$$

$$C_A(+\infty, y, z) = C_A(x, \pm\infty, z) = C_A(x, y, 0) = C_A^\circ$$

$$\frac{\partial C_A}{\partial z}(x, y, M) = 0 \text{ in "acceptor region" (no flux condition)}$$

$$C_A(x, y, z) = 0 \text{ in "donor region"}$$

In addition, boundary conditions for the interface between EA and ED (Figure 3.1) have to be specified. It is to be noted that the position of this interface is unknown a priori and will be determined in section 3.2.3. Due to the assumption of an entire consumption of donor and acceptor at the interface, the following boundary conditions apply at the plume fringe:

$$C_D(x, y, z) = C_A(x, y, z) = 0$$

where x, y and z are the Cartesian coordinates as depicted in Figure 3.1. C_D° and C_A° are the source concentrations [ML^{-3}] of ED and EA, respectively. D_D and D_A are molecular diffusion coefficients [L^2T^{-1}] for ED and EA, respectively, and α_L, α_{Th} and α_{Tv} are dispersivities [L] in longitudinal, transverse horizontal and transverse vertical directions, respectively. γ is a dimensionless number called utilization factor (*Wiedemeier et al.*, 1999, p. 196). It is the product of the stoichiometric ratio of EA and ED and the molecular weight ratio of EA and ED . r is a reaction rate [$ML^{-3}T^{-1}$], which is zero in the entire domain except at the plume fringes. The diffusion coefficients for both the EA and the ED are assumed to be equal for the modeled case. Thus, a single diffusion coefficient, D, can be used to represent both diffusion coefficients, i.e., $D_D = D_A = D$. Next, we introduce the variable $C(x, y, z) = \gamma C_D(x, y, z) - C_A(x, y, z)$, which represents the deficit in EA concentration as compared to the concentration actually needed in

the reaction to achieve a complete consumption of the ED. After multiplying eq. (3.1) with γ and subtracting eq. (3.2) from it, a single transport equation (3.3) is obtained for C:

$$v\frac{\partial C}{\partial x} - (\alpha_L v + D)\frac{\partial^2 C}{\partial x^2} - (\alpha_{Th} v + D)\frac{\partial^2 C}{\partial y^2} - (\alpha_{Tv} v + D)\frac{\partial^2 C}{\partial z^2} = 0 \tag{3.3}$$

with the following boundary conditions:

$$C(0, y, z) = \begin{cases} \gamma C_D^\circ & \text{if } -W \leq y \leq +W \\ -C_A^\circ & \text{else} \end{cases}$$

$$C(+\infty, y, z) = C(x, \pm\infty, z) = C(x, y, 0) = -C_A^\circ$$

$$\frac{\partial C}{\partial z}(x, y, M) = 0$$

Dividing by v results in D/v terms appearing in eq. (3.3). The D/v ratio can be safely assumed to be much smaller than any dispersivity used in eq. (3.3), and therefore, this ratio can be omitted from the equation. α_L has been found to have very small or almost no effect on the plume length, e.g., by *Ham et al.* (2004), *Liedl et al.* (2005). Therefore, the term with α_L can also be neglected in eq. (3.3). Finally, the following model equation(3.4) result that has identical boundary conditions as eq. (3.3):

$$\frac{\partial C}{\partial x} - \alpha_{Th}\frac{\partial^2 C}{\partial y^2} - \alpha_{Tv}\frac{\partial^2 C}{\partial z^2} = 0 \tag{3.4}$$

It is important to comment on the assumptions made on diffusion coefficients in the formulation of model equation (3.4) and in specifying them in the domain. The elimination of diffusion coefficients from eq. (3.3) ideally makes the model equation independent of flow velocity, which in turn makes the proposed model valid for any flow condition. The solution of the model equation (see subsections 3.2.2 and 3.2.3) is found to be independent of diffusion coefficients, implying that these parameters can be simply added to the dispersivities in the final model solution if their impacts are to be determined. More critical, rather, is the assumption of the equal diffusion coefficients of EA and ED in the domain. A very recent work by *Chiogna et al.* (2010) has shown that diffusion coefficients are chemical specific. If different diffusion coefficients are to be considered for EA and ED, then the approach used in formulation of eq. (3.3), and the entire method adopted in this chapter to solve the model equation, need to be changed.

3.2.2 Concentration Profiles

Observing the boundary conditions at $z = 0$ (fixed concentration) and $z = M$ (no mass flux), the concentration $C(x, y, z)$ can be written as an infinite sine series:

$$C(x,y,z) = (\gamma C_D^\circ + C_A^\circ) \sum_{n=1}^{\infty} \left[b_n(x,y) \sin(2n-1)\frac{\pi z}{2M} \right] - C_A^\circ \tag{3.5}$$

where the coefficients b_n remain to be determined. This approach is adopted from *Carslaw and Jaeger* (1959, p. 97, eq. 8), who studied a mathematically similar heat flow problem, and generalizes the solution technique already used by *Liedl et al.* (2005). By inserting eq. (3.5) into eq. (3.4), it can be shown that each coefficient $b_n(x, y)$ must satisfy the corresponding second-order differential equation

$$\frac{\partial b_n}{\partial x} - \alpha_{Th}\frac{\partial^2 b_n}{\partial y^2} + \alpha_{Tv}(2n-1)^2\left(\frac{\pi}{2M}\right)^2 b_n = 0 \tag{3.6}$$

with the following boundary conditions:

$$b_n(x, \pm\infty) = 0 \quad \text{and}$$

$$\sum_{n=1}^{\infty} b_n(0,y) \sin(2n-1)\frac{\pi z}{2M} = \left\{ \begin{array}{ll} 1 & \text{if } -W \le y \le +W \\ 0 & \text{else} \end{array} \right\} = H(y+W) - H(y-W) \tag{3.7}$$

where H is the Heaviside function, which is the unit step function that equals unity for positive and zero for negative arguments. Applying an inversion formula from *Bronshtein and Semendyayev* (1997, p. 575, eq. 5) (for details see Appendix 2), the following expression for $b_n(0, y)$ is obtained:

$$b_n(0,y) = \frac{4}{\pi}\frac{1}{2n-1}\Big[H\big(y+W\big) - H\big(y-W\big)\Big] \tag{3.8}$$

In order to solve eq. (3.6), it is most convenient to remove the third term on the left hand side by applying the approach

$$b_n(x,y) = a_n(x,y)\, e^{-\alpha_{Tv}(\frac{\pi}{2M})^2(2n-1)^2 x} \tag{3.9}$$

where the unknown function, a_n, obeys the same boundary conditions as b_n.

Inserting eq. (3.9) into eq. (3.6) transforms it to

$$\frac{\partial a_n}{\partial x} - \alpha_{Th}\frac{\partial^2 a_n}{\partial y^2} = 0 \tag{3.10}$$

From *Crank* (1976), the solution for a_n is obtained as

$$a_n(x,y) = \frac{2}{\pi}\frac{1}{(2n-1)}\left(\operatorname{erf}\frac{y+W}{\sqrt{4\alpha_{Th}x}} - \operatorname{erf}\frac{y-W}{\sqrt{4\alpha_{Th}x}}\right) \tag{3.11}$$

Substituting a_n from eq. (3.11) into eq. (3.9) provides the solution for $b_n(x,y)$ as

$$b_n(x,y) = \frac{2}{\pi}\frac{1}{(2n-1)}\left(\operatorname{erf}\frac{y+W}{\sqrt{4\alpha_{Th}x}} - \operatorname{erf}\frac{y-W}{\sqrt{4\alpha_{Th}x}}\right).e^{-\alpha_{Tv}\left(\frac{\pi}{2M}\right)^2(2n-1)^2x} \tag{3.12}$$

Finally substituting b_n into eq. (3.5), the solution for the concentration profile in 3D is obtained as

$$\begin{aligned} C(x,y,z) \;=\; & \frac{2}{\pi}(\gamma C_D^\circ + C_A^\circ)\left(\operatorname{erf}\frac{y+W}{\sqrt{4\alpha_{Th}x}} - \operatorname{erf}\frac{y-W}{\sqrt{4\alpha_{Th}x}}\right). \\ & .\sum_{n=1}^{\infty}\left[\frac{1}{(2n-1)}e^{-\alpha_{Tv}\left(\frac{\pi}{2M}\right)^2(2n-1)^2x}\sin(2n-1)\frac{\pi z}{2M}\right] - \\ & -C_A^\circ \end{aligned} \tag{3.13}$$

As $C(x,y,z) = \gamma C_D(x,y,z)$ in the donor region ($C_A = 0$), we get

$$\begin{aligned} C_D(x,y,z) \;=\; & \frac{2}{\pi}(C_D^\circ + \frac{C_A^\circ}{\gamma})\left(\operatorname{erf}\frac{y+W}{\sqrt{4\alpha_{Th}x}} - \operatorname{erf}\frac{y-W}{\sqrt{4\alpha_{Th}x}}\right). \\ & .\sum_{n=1}^{\infty}\left[\frac{1}{(2n-1)}e^{-\alpha_{Tv}\left(\frac{\pi}{2M}\right)^2(2n-1)^2x}\sin(2n-1)\frac{\pi z}{2M}\right] - \\ & -\frac{C_A^\circ}{\gamma} \end{aligned} \tag{3.14}$$

for the electron donor and, similarly,

$$C_A(x,y,z) = C_A^\circ - \frac{2}{\pi}(\gamma C_D^\circ + C_A^\circ)\Big(\operatorname{erf}\frac{y+W}{\sqrt{4\alpha_{Th}x}} - \operatorname{erf}\frac{y-W}{\sqrt{4\alpha_{Th}x}}\Big). \cdot\sum_{n=1}^{\infty}\Big[\frac{1}{(2n-1)}e^{-\alpha_{Tv}\left(\frac{\pi}{2M}\right)^2(2n-1)^2x}\sin(2n-1)\frac{\pi z}{2M}\Big] \quad (3.15)$$

in the acceptor region where $C_D = 0$ and, consequently, $C(x,y,z) = -C_A(x,y,z)$.

3.2.3 Concentration Isosurfaces and Plume Length

In the earlier 2-D models, for example by *Ham et al.* (2004), *Liedl et al.* (2005), the explicit formula for the plume length was provided for the distance between the source and the point where the ED concentration is zero. However, for practical applications, zero concentrations of contaminant are often not required. Legislatively defined concentrations such as threshold concentrations often become a target concentration in the plume profile. Hence, an ED concentration C_D^{thres} with $0 \le C_D^{thres} \le C_D^\circ$ is introduced. The eq. (3.14) can then be rearranged to express the corresponding threshold ED concentration isosurface as

$$\frac{\pi}{2}\frac{\gamma C_D^{thres} + C_A^\circ}{\gamma C_D^\circ + C_A^\circ} = \Big(\operatorname{erf}\frac{y+W}{\sqrt{4\alpha_{Th}x}} - \operatorname{erf}\frac{y-W}{\sqrt{4\alpha_{Th}x}}\Big). \cdot\sum_{n=1}^{\infty}\Big[\frac{1}{(2n-1)}e^{-\alpha_{Tv}\left(\frac{\pi}{2M}\right)^2(2n-1)^2x}\sin(2n-1). \cdot\frac{\pi z}{2M}\Big] \quad (3.16)$$

It is to be noted that when $C_D^{thres} = 0$, the position of the plume fringe is obtained from eq. (3.16). Furthermore, as the contaminant source is assumed to extend over the entire aquifer thickness, the maximum travel distance of ED (plume length) will be reached at the bottom of the aquifer due to the impervious boundary and due to the supply of EA from the top. In order to derive an expression for the plume length it is therefore necessary to quantify ED concentration isolines at the aquifer bottom. This can be directly achieved by setting $z = M$ in eq. (3.16), where M represents the actual thickness of the aquifer and the source. Additionally, when $\sin(2n-1)\pi/2$ is replaced with $(-1)^{n-1}$, eq. (3.16) simplifies

to a concentration contour at the bottom of the aquifer as in

$$\frac{\pi}{2}\frac{\gamma C_D^{thres}+C_A^{\circ}}{\gamma C_D^{\circ}+C_A^{\circ}}=\left(\operatorname{erf}\frac{y+W}{\sqrt{4\alpha_{Th}x}}-\operatorname{erf}\frac{y-W}{\sqrt{4\alpha_{Th}x}}\right)\cdot\sum_{n=1}^{\infty}\frac{(-1)^{n-1}}{(2n-1)}e^{-\alpha_{Tv}\left(\frac{\pi}{2M}\right)^2(2n-1)^2x} \tag{3.17}$$

Furthermore, due to symmetry of the model set-up in $y-$direction, the maximum plume extension is found for $y=0$. As a result, both erf terms in eq. (3.17) can be added and the centerline plume length, L replacing x, is then given by:

$$\operatorname{erf}\frac{W}{\sqrt{4\alpha_{Th}L}}\cdot\sum_{n=1}^{\infty}\frac{(-1)^{n-1}}{(2n-1)}e^{-\alpha_{Tv}\left(\frac{\pi}{2M}\right)^2(2n-1)^2L}=\frac{\pi}{4}\frac{\gamma C_D^{thres}+C_A^{\circ}}{\gamma C_D^{\circ}+C_A^{\circ}} \tag{3.18}$$

Eq. (3.18) represents an implicit expression for L, appearing in an infinite number of terms. *Liedl et al.* (2005) analyzed this series and showed that absolute differences in plume length are on the order of 10^{-7} when using either only the first or 25 terms of this series. The final plume length equation is therefore given by

$$\operatorname{erf}\frac{W}{\sqrt{4\alpha_{Th}L_1}}\cdot e^{-\alpha_{Tv}\left(\frac{\pi}{2M}\right)^2L_1}=\frac{\pi}{4}\frac{\gamma C_D^{thres}+C_A^{\circ}}{\gamma C_D^{\circ}+C_A^{\circ}} \tag{3.19}$$

where L_1 refers to the plume length obtained by considering only the first term of the infinite series in eq. (3.18). Eq. (3.19) can be seen as an expression containing three parameter groups: the lateral source dimension (W) and the corresponding horizontal mixing parameter (α_{Th}), the vertical source dimension (M) and the corresponding vertical mixing parameter (α_{Tv}) and the so called chemical term, which includes all relevant chemical parameters (C_D°, C_A°, C_D^{thres} and γ). This term can only take values between 0 and $\pi/4 \approx 0.78$. In the works of *Ham et al.* (2004) and *Maier and Grathwohl* (2006) for example, values lower than 0.2 were used for the chemical term, although in those works the chemical term does not include a C_D^{thres} component, which can slightly increase its overall value. To the best knowledge of the authors the value of the chemical term never exceeds 0.5 in practically relevant cases. Also, the erf term on the left hand side of eq. (3.19) will be equal to unity when the argument of erf becomes greater than or equal to 2. In that case, the model equation (3.19) will be identical to the 2D analytical model suggested by *Liedl et al.* (2005). In order to understand the impacts of a finite source width and the horizontal transverse dispersivity (α_{Th}) on the plume length, it is important to preserve all terms of eq. (3.19) in the solution. This necessitates numerical solution of eq. (3.19). Details of the

numerical approach are provided in Appendix 2.

3.3 3D Model Results, Evaluation and Discussion

In this section the expression for the plume length (eq. 3.19) obtained in the section 3.2.3 is analyzed. The data used in analyses (provided in table 3.1) are not specific to any site but they correspond to the range of data (from mostly petroleum hydrocarbon sites undergoing aerobic biodegradation) summarized in *Wiedemeier et al.* (1999) or suggested in the manual of the BIOSCREEN model. Scenarios that are not very practical, e.g., where $\alpha_{Tv} > \alpha_{Th}$ or where $M > W$, are also used to complement the analyses. The source dimensions and the dispersivities are considered the primary variables in the analyses. Chemical parameters are mostly left constant. This is basically from the results of *Liedl et al.* (2005), on which the 3D model is based, in which it was shown that the chemical parameters are relatively less significant than the source dimension or dispersivity for plume length estimations in the 2D domain. For the analyses, the numerical solution of the 3D expression (eq. 3.19) was first implemented in an Excel^{TM} spreadsheet, which was then used to simulate different scenarios described in this section.

3.3.1 Comparing the 3D model with the 2D model

Theoretically, the only difference between the 2D model of *Liedl et al.* (2005) and the 3D model (eq. 3.19) is the presence of the finite lateral source extension in the 3D model. The consequence of this difference, which is mathematically represented by the erf term in eq. (3.19), is the existence of additional degradation surfaces resulting in shorter plumes. In case of large plume width ($2W >> M$), however, the effect of lateral mixing is minor, the erf term approaches unity and the plume length (L_1) can be obtained according to the 2D model from

$$L_1 = \frac{4}{\pi^2}\frac{M^2}{\alpha_{Tv}} \ln\left(\frac{4}{\pi}\frac{\gamma C_D^{\circ} + C_A^{\circ}}{\gamma C_D^{thres} + C_A^{\circ}}\right) \tag{3.20}$$

If the source width is comparable to or smaller than the source thickness, the erf term in eq. (3.19) assumes a value smaller than 1. In this case, the argument of the erf term is smaller than 2. Based on this, a relevant source width ($2W_{rel}$) is defined, such that the 2D model is sufficient if $2W > 2W_{rel}$, by setting

$$2W_{rel} = 8\sqrt{\alpha_{Th} L_1} \tag{3.21}$$

Table 3.1: Model Parameters and Values Used in the Simulations.

Parameter	Range	Unit
Electron Acceptor Concentration, (C_A°)	8	mg/L
Electron Donor Concentration, (C_D°)	15	mg/L
Electron Donor Threshold Concentration, (C_D^{thres})	0.005	mg/L
Mass Ratio, (γ)	3.5	
Vertical Transverse Dispersivity, (α_{Tv})	0.01–50	mm
Horizontal Transverse Dispersivity, (α_{Th})	10*α_{Tv}	mm
Source Width, ($2\,W$)	0–30	m
Aquifer and Source Thickness, (M)	0–25	m

Here, L_1 can be replaced with the right hand side of eq. (3.20), because in this particular case the 3D expression is practically identical with the 2D expression. This leads to

$$2W_{rel} = \frac{16M}{\pi}\sqrt{\frac{\alpha_{Th}}{\alpha_{Tv}}\ln\left(\frac{4}{\pi}\frac{\gamma C_D^\circ + C_A^\circ}{\gamma C_D^{thres} + C_A^\circ}\right)} \tag{3.22}$$

Eq. (3.22) provides $2W_{rel}$ as a function of dispersivity ratio, chemical parameters and the source thickness. For practical purposes, a plot (Figure 3.2) of $2W_{rel}/M$ as a function of the chemical parameters quantifies limits for the relevance of the 3D or the 2D model for various dispersivity ratios. Figure 3.2 indicates that the 3D model is to be used only if $2W/M$ is below the appropriate dispersivity ratio curve.

Figure 3.3 compares plume lengths obtained from the 3D model and the 2D model for different M at a fixed dispersivity ratio ($\alpha_{Th}/\alpha_{Tv} = 10$) and at a fixed chemical condition ($\frac{\pi}{4}\frac{\gamma C_D^{thres}+C_A^o}{\gamma C_D^\circ+C_A^o} = 0.1$, see Table 3.1) but at varying source widths. The obtained results (Figure 3.3) very clearly show a linearly increasing ratio of plume lengths (L_{2D}/L_{3D}) with increasing M for any tested W. However, the slopes are found to decrease with increasing W, and the decreasing trend of the slopes suggest that at some very large W the two models will provide identical results for the plume length. The source width at which both models will predict an identical result is $2W_{rel}$ and its value can be obtained from eq. (3.22). *Wiedemeier et al.* (1999) suggests that the source width does not exceed very much over 5 times the thickness. In such cases the 3D model is likely to predict significantly shorter plume lengths, up to 3 times in the tested cases, than the 2D model.

The 2D and 3D models are further compared for different dispersivities in Figure 3.3. In this case the source width is fixed (i.e., $2W = 10$ m) in addition to the fixed dispersivity ratio and the chemical condition as defined above. The

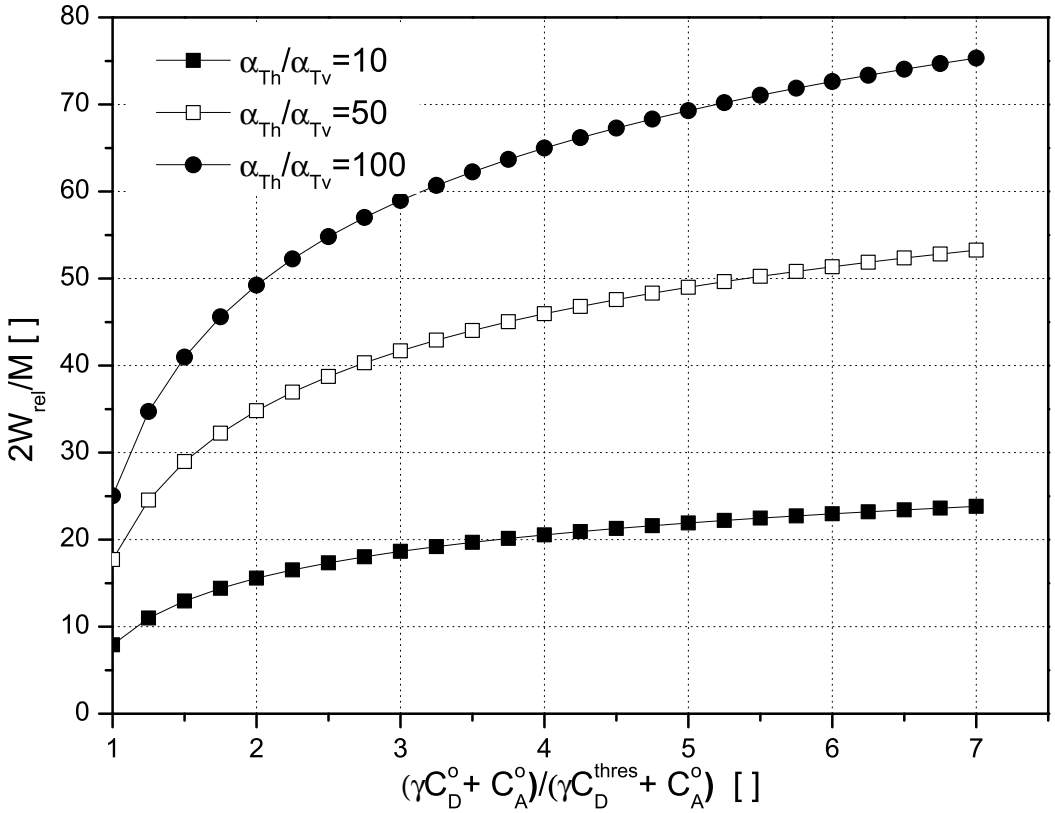

Figure 3.2: $2W_{rel}/M$ at different chemical conditions for different dispersivity ratios.

obtained results again provide significantly shorter plume lengths from the 3D model as compared to the 2D model. The results also suggest that the effects of dispersivity are reduced with the decreasing source thicknesses. Database studies on plume length of hydrocarbon contaminated sites (e.g., *Teutsch et al.*, 1997) provide an average plume length of less than hundred meters. Very similar results can be observed from the 3D model in Figure 3.3 when $\alpha_{Tv} = 50$ mm. The effect of different dispersivity ratios ($\alpha_{Th}/\alpha_{Tv} = 10 - 50$) on the plume length was also investigated. The results (not provided here) of that comparison provided higher differences in plume lengths at increasing dispersivity ratios. It is likely that the significance of either of the dispersivities is related to the source dimensions.

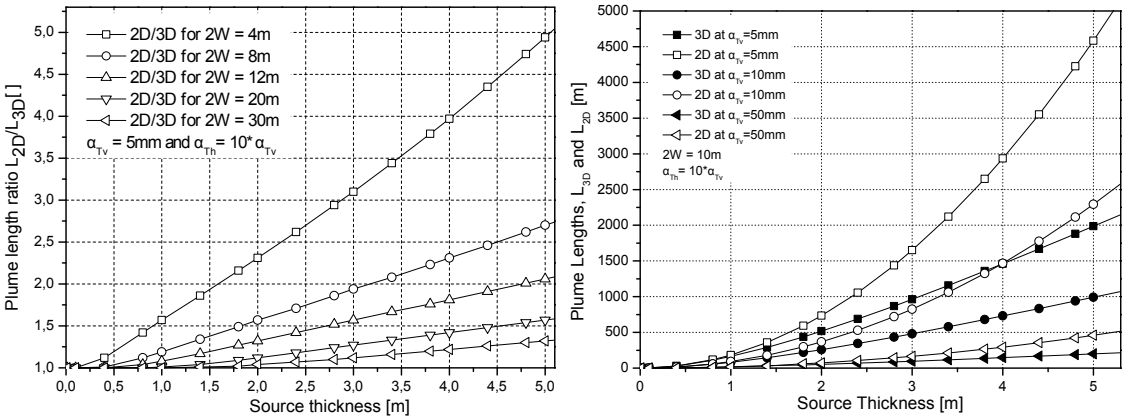

Figure 3.3: Plume length from the 2D and the 3D models as a function of source thickness (M) and at fixed chemical condition (see Table 3.1) Left figure- dispersivitiy is constant and the source width (2W) is veried. Right figure- source width(2W) is held constant and dispersivity is veried.

3.3.2 Impact of the Source Shape on Plume Length

The importance of the source geometry was realized in the subsection above. The 3D model requires that the source dimensions ($2*W$ and M) be finite. Therefore, it is possible to analyze impacts of the different source geometries on the plume length with this model. For that purpose, the plume length is plotted as a function of the source dimension ratio (M/W, see Figure 3.4) at different dispersivity ratios and at the fixed chemical condition (data provided in Table 3.1). Furthermore, the ratios of the source dimensions are set in such a way that their products are always constant (i.e., $M*2W = 50$ m^2). This arrangement eliminates the impact of varying source volume per unit length on the plume length. Additionally, for the M/W ratio, M increases from 1 m to 25 m from left to right along the x-axis of Figure 3.4 and accordingly, W decreases from 25 m to 1 m from right to left. This enables the association of the left end of the x-axis with a very narrow column-like source, likewise the right end of the axis represents a very wide source. The dispersivity ratios provide α_{Tv} and α_{Th} varying between 0.1 cm to 5 cm and 1 cm to 50 cm, respectively. The highest dispersivity ratio results from a combination of the lowest α_{Tv} and the highest α_{Th}. The obtained results (see Figure 3.4) clearly provide largest plume lengths (L_{max}) at dispersivity ratios that are more often observed in the field (i.e., $\alpha_{Th}/\alpha_{Tv} > 10$) for source dimensions with $M/W \approx 1$ or log(M/W) ≈ 0. Plume lengths are also observed to rapidly decrease from L_{max} when M and W are not approximately equal in those dispersivity ratios. For less likely dispersivity ratios, $\alpha_{Th}/\alpha_{Tv} < 10$, the L_{max} is found to shift

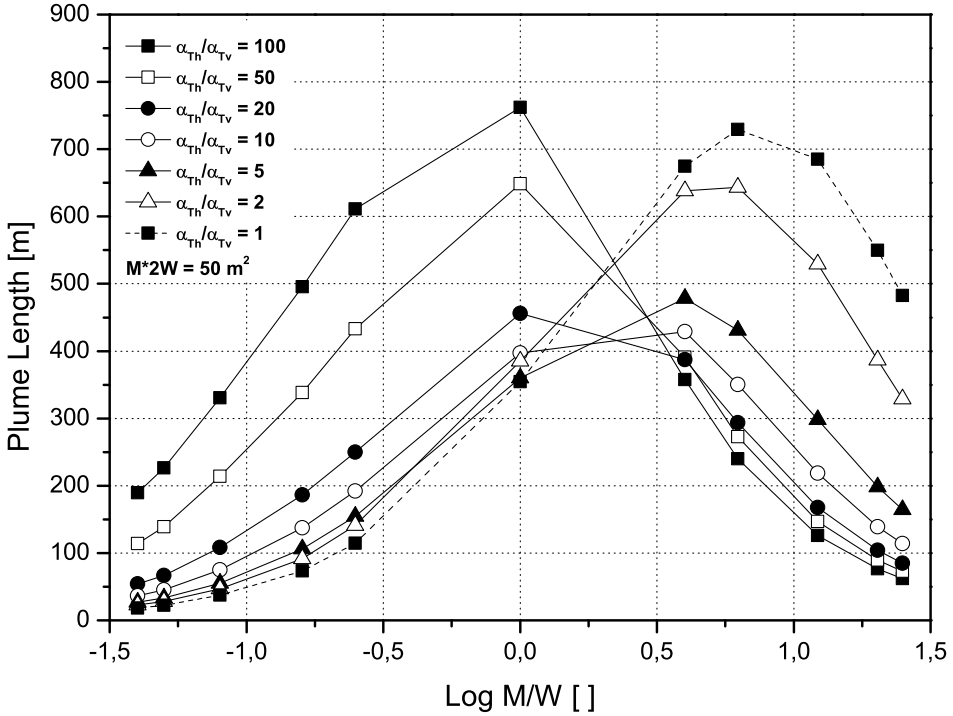

Figure 3.4: Plume length as a function of source thickness (M) to width (W) ratio at varying dispersivity ratios (α_{Th}/α_{Tv}). M increases and W accordingly decreases from left to right along the x-axis.

towards the $M > W$ zone. Additionally, the figure clearly shows the importance of different dispersive mixing for varying source dimensions. In the M dominating regions shorter plume lengths result at higher α_{Th}. Likewise, in the zone where W dominates shorter plume lengths results at higher α_{Tv}. These effects can be explained by interplay between source geometry and mixing of reactants. Narrow plume emerges for $M >> W$ as in these cases lateral surfaces are much larger than the top surface. In such cases lateral mixing is more effective in reducing the plume length than vertical mixing. The opposite is true for shallow sources ($M << W$). The influence of source dimensions and shape is further examined by performing sensitivity analyses in the next subsection.

3.3.3 Comparing the Influence of the 3D Model Parameters on Plume Length

The influence of source's geometry on plume length was studied in the subsection above. Sensitivity analyses, using the relative sensitivity coefficient (S_{rel}) as described by *Zheng and Bennett* (2002), are performed here to identify which combinations of source dimension and dispersivity are more influential on the plume length than others. The following three scenarios are considered: $M > W$, $M = W$ and $M < W$. For all of the three scenarios the same chemical condition, as in the previous subsections, and dispersivity ratios (Figure 3.5) were used. The obtained results (left, Figure 3.5), clearly suggest that the combination of M and α_{Th} (more negative S_{rel}) will be more influential on plume length than the combination of W and α_{Tv} if $M > W$. The opposite is true when W is larger than M. The obtained results from the sensitivity analyses complement the explanations that were provided on the results observed in Figure 3.4 in the previous subsection. Chemical parameters were not used in the sensitivity analyses largely because these parameters were found to be less influential on plume length when compared to dispersivity and source dimensions in *Liedl et al.* (2005).

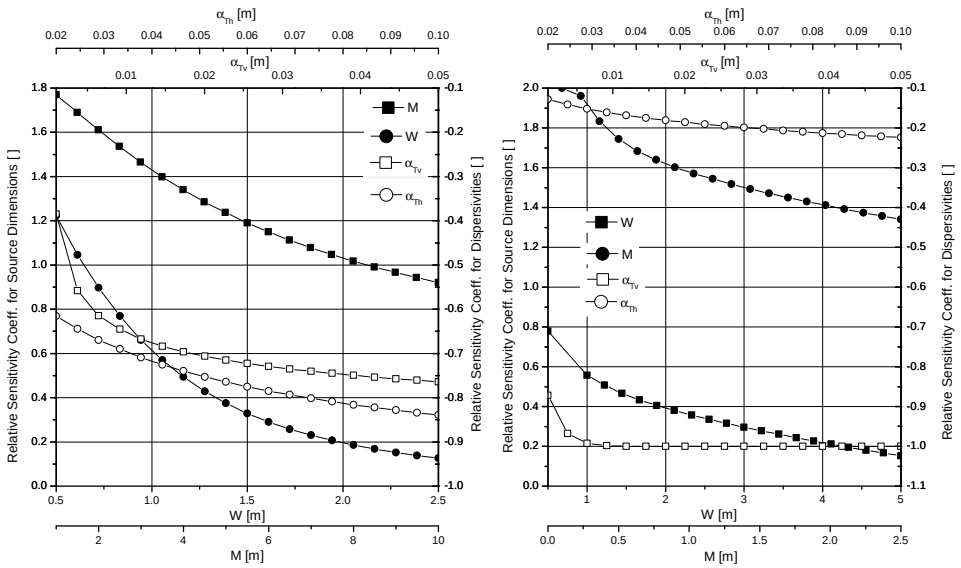

Figure 3.5: Relative sensitivity coefficients of the parameters of the 3D model. Higher relative sensitivity coefficients refer to higher influence of that parameter on the plume length. The plot on the left is for the $M > W$ case and the plot on the right is for the $W > M$ case.

3.4 Conclusions

In general, the 3D analytical expression, which represents an extension of earlier work by *Liedl et al.* (2005), can be used to estimate the steady state (or maximum) length of contaminated plumes. For easier calculations, the 3D solution is implemented in an Excel^{TM} spreadsheet. Initial results for theoretical cases were shown to significantly reduce the exponential increase of plume lengths with source thicknesses, which is generally predicted by 2D models. Theoretical comparisons with the 2D model of *Liedl et al.* (2005) suggest the divergence point between these two models for any finite source dimensions to be a combined function of dispersivities and chemical conditions in the aquifer. A relationship for the source dimensions is developed to determine when the 2D model is sufficient to estimate plume lengths. The plume lengths were also shown to be dependent on the shape of the source. In general, sources with approximately square shape are associated with maximum plume length at any dispersivity ratio bigger than 10 (i.e., $\alpha_{Th}/\alpha_{Tv} > 10$). Shorter plume lengths result when source width and thickness are different. Through sensitivity analyses it was clarified that the longitudinal extensions of plumes, obtained using the model developed in this chapter, is influenced more by the combination of longer source dimension (M or W) and the transverse dispersivity in the direction of shorter source dimension (α_{Tv} or α_{Th}).

Chapter 4

Influence of Source Thickness on Steady-State Plume Length

4.1 Introduction

[3] In recent years several analytical models, encompassing several contaminated site scenarios, have been suggested to predict mixing controlled longitudinal extension of the plume. *Liedl et al.* (2005, 2011) provide expressions for estimating steady-state plume length for the fully penetrating contaminant source in a 2D and a 3D domain, respectively. From the expressions provided in *Cirpka and Valocchi* (2007) and *Cirpka* (2010), in which the source is horizontally oriented in a 2D domain, the bio-chemically limited extension of plumes can be estimated. Further approaches to estimate steady-state plume length for horizontal scenarios were provided by *Ham et al.* (2004) and *Chu et al.* (2005). The major advantage of these models, e.g., when used as a pre-assessment tool for contaminated site management, is the small number of parameters required. However, despite the straightforward application, these models are subject to several limitations. Among others, it is either explicitly or directly assumed that the vertical source extension coincides with aquifer thickness.

This chapter is designed to test the applicability of the analytical models of *Liedl et al.* (2005, 2011) for contaminant sources not extending to the aquifer bottom (partly penetrating source). To this end, analytical predictions are compared to numerical results obtained by solving the transformed advection-dispersion equation already used in *Liedl et al.* (2005, 2011).

[3] This chapter has been submitted to Water Resour. Res., as: Yadav, P. K., R. Liedl., and P. Dietrich, (2012), Influence of Source Thickness on Steady-State Plume Length.

4.2 Theoretical Background

4.2.1 Model Set-up

Considered here is a saturated homogeneous aquifer with a uniform horizontal flow field (v, [LT^{-1}]) and uniformly distributed contaminated source (referred to as Electron Donor or ED) with concentration C_D, [ML^{-3}]. According to Figure 4.1, the source extends across the rectangle $-W \leq y \leq +W$ and $0 \leq z \leq M_s$ such that source depth M_s is smaller than aquifer depth M. Contaminant spreading

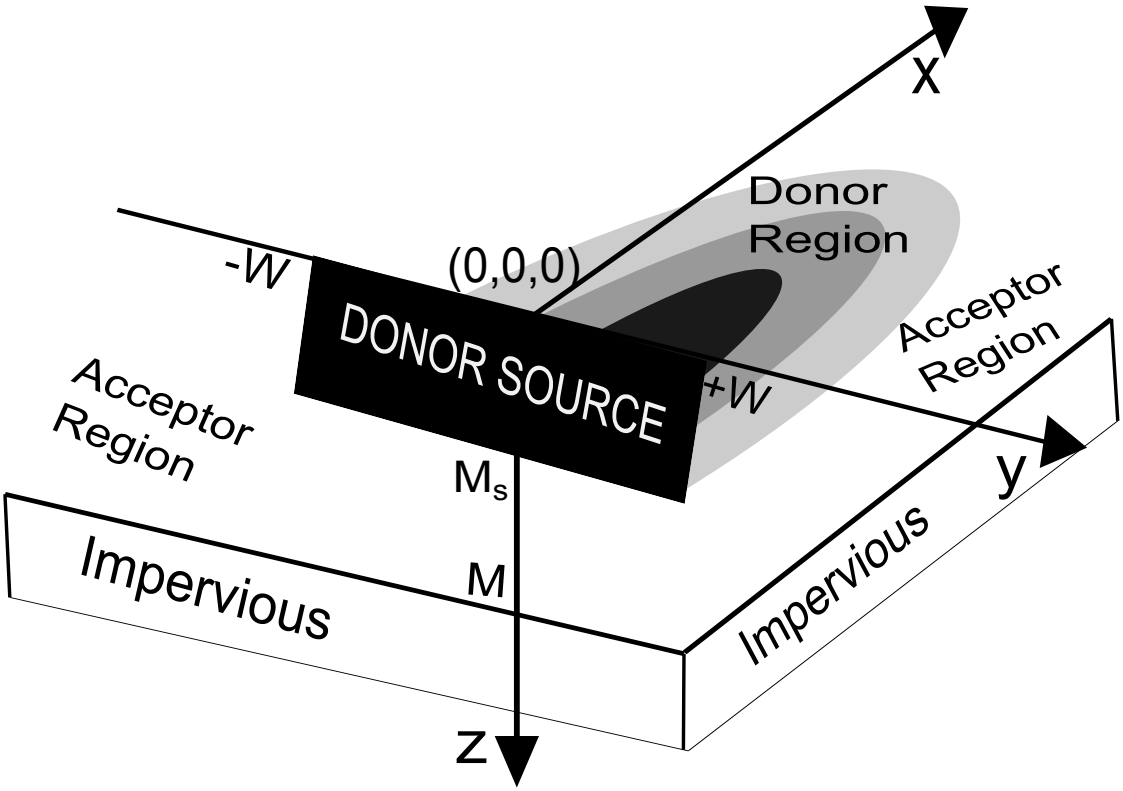

Figure 4.1: The basic model set-up.

is limited by a binary-type reaction involving an Electron Acceptor (EA) with uniform concentration C_A [ML^{-3}], at the aquifer top and at the inflow boundary ($x = 0$) not occupied by the source. An instantaneous reaction between ED and EA is assumed to occur along the fringe of the plume.

This 3D set-up simplifies to a 2D scenario in case of "large" source width ($2W \to +\infty$). The transport model, without any sorption, for both ED and EA

can be written as:

$$\phi_e \frac{\partial C_{D,A}}{\partial t} + \nabla \cdot (\phi_e v\, C_{D,A} - \phi_e D\, \nabla\, C_{D,A}) = -\gamma_A r \tag{4.1}$$

in which the subscripts D and A refer to ED or EA, respectively. $D = \alpha_i\, v + D_p$ is hydrodynamic dispersion [L^2T^{-1}], with subscript i referring to L, Th and Tv in order to represent dispersivity [L] in longitudinal, transverse horizontal and transverse vertical directions, respectively. ϕ_e [-] is effective porosity, D_p [L^2T^{-1}] is pore diffusion coefficient, and r [$ML^{-3}T^{-1}$] is the reaction rate that has a positive value at the fringes of the plume and is zero elsewhere. γ [-] is the utilization factor of the binary reaction as defined in *Wiedemeier et al.* (1999). As in both Liedl et al. models, both α_L and D_p are neglected and a steady-state is considered. Additional mathematical details of model formulation including boundary conditions can be found in *Liedl et al.* (2005, 2011).

A very important aspect of the Liedl et al. works is the mathematical transformation of eq. (4.1) that leads to a single transport equation in terms of a new concentration $C = \gamma C_D - C_A$, representing the EA deficit. This equation results from the multiplication of the ED equation with γ and then subtracting the EA equation from it:

$$\phi_e \frac{\partial C}{\partial t} + \nabla \cdot (\phi_e v\, C - \phi_e D\, \nabla\, C) = 0 \tag{4.2}$$

The transformed equation is independent of the reaction rate. The solution includes the position in the domain where $C = 0$, i.e., the fringe of the plume. Positive results ($C > 0$) correspond to donor concentrations $C_D = C/\gamma$, whereas negative values $C < 0$ represent acceptor concentrations $C_A = -C$. In the rest of this chapter, the transformed model equation will be used.

4.2.2 Steady-State Plume Fringe Location

For the fully penetrating source ($M_s = M$), *Liedl et al.* (2011) provide an implicit expression for the steady-state isosurface $C = 0$ representing the maximum extension of the plume (3D approach):

$$\begin{aligned} \frac{\pi}{2} \frac{C_A^\circ}{\gamma C_D^\circ + C_A^\circ} \;=\; & \left(\operatorname{erf} \frac{y + W}{\sqrt{4 \alpha_{Th} x}} - \operatorname{erf} \frac{y - W}{\sqrt{4 \alpha_{Th} x}} \right) \cdot \\ & \cdot \sum_{n=1}^{\infty} \left[\frac{1}{(2n-1)} e^{-\alpha_{Tv} \left(\frac{\pi}{2M} \right)^2 (2n-1)^2 x} \cdot \sin(2n-1) \frac{\pi z}{2M} \right] \end{aligned} \tag{4.3}$$

For reasons of symmetry, the maximum extension of the plume in flow direction (plume length) is reached along the centerline ($y = 0$). Further, *Liedl et al.* (2005, 2011) showed that plume length may be very well approximated by considering only the first term in the series appearing on the right-hand side of eq. (4.3). From this, we obtain an expression for the plume fringe location in the plane $y = 0$:

$$\frac{\pi}{4}\frac{C_A^\circ}{\gamma C_D^\circ + C_A^\circ} = \operatorname{erf}\frac{W}{\sqrt{4\alpha_{Th}x}} \cdot e^{-\alpha_{Tv}\left(\frac{\pi}{2M}\right)^2 x} \cdot \sin\frac{\pi z}{2M} \tag{4.4}$$

which can be solved for $\frac{z}{M}$, yielding

$$\frac{z}{M} = \frac{2}{\pi}\arcsin\left[\frac{\frac{\pi}{4}\frac{C_A^\circ}{\gamma C_D^\circ + C_A^\circ}}{\operatorname{erf}\frac{W}{\sqrt{4\alpha_{Th}x}}} \cdot e^{\alpha_{Tv}\left(\frac{\pi}{2M}\right)^2 x}\right] \tag{4.5}$$

For the partly penetrating source, we set $z = M_s$ in eq. (4.5) and then solve for x to obtain an approximation of plume length (L). This approach involves a rather critical assumption that the most downgradient point of the plume fringe is located at the level $z = M_s$. This assumption is a consequence of using only the first term of the infinite series of eq. (4.3). Results, obtained from solving eq. (4.5) and eq. (4.6), will be compared in section 4.3 with isosurface locations obtained by numerically solving eq. (4.2). It should be added that an explicit solution of eq. (4.5) is possible for the vertical 2D scenario (large source width) as the error function tends to unity in this case. Plume length is then estimated as:

$$x = L = \left(\frac{2M}{\pi}\right)^2 \frac{1}{\alpha_{Tv}} \ln\left[\frac{4}{\pi}\frac{\gamma C_D^\circ + C_A^\circ}{C_A^\circ} \cdot \sin\left(\frac{\pi}{2}\frac{M_s}{M}\right)\right] \tag{4.6}$$

4.3 Influence of Source Thickness

4.3.1 The 2D case

Numerical experiments will be performed first to find the plume lengths resulting from different M_s/M ratios. Later, the numerically obtained plume lengths are to be compared with analytical results from eq. 4.6. For the numerical experiments Comsol Multiphysics® modeling environment is used. The modeling domain is set similar to Figure 4.1 but restricted to the 2D strip defined by $x > 0$, $y = 0$ and $0 < z < M$. The longitudinal extension is initially set to one and half times larger than the plume lengths resulting from *Liedl et al.* (2005) analytical expression and it is readjusted if required. The source thickness, equaling to aquifer thickness ($M = M_s$) for validation purposes is set to 1 m, 3 m and 7 m for the first three different simulations. The boundary conditions for the numerical domains are set

in the following way: the constant concentration ED at the inflow boundary on the left of the domain is set to $\gamma * C_D$ = 3.5 x 15 mg/L, whereas the constant concentration for the EA at the top of the domain, at the outflow boundary, and at the part of the inflow boundary not occupied by the source is set to $-C_A = -8$ mg/L. The bottom of the domain is impervious (no-flow boundary). Transverse vertical dispersivity (α_{Tv}) is set to 5 cm and the groundwater velocity is 0.85 m/d. The selected value of the parameters are obtained from literature, e.g., *Liedl et al.* (2011). Due to limited scope of this chapter, all parameters except M are kept unchanged. As mentioned earlier, the required solution is the zero concentration isoline and the plume length is the maximum longitudinal extension of that isoline. The results from the numerical experiment are provided in Figure 4.2. From the figure it is clear that for the source thickness equaling the aquifer depth (in the figure at M_s/M=100%), both the numerical and analytical results are almost identical for all three considered cases. This validates the numerical code for the considered scenario.

Next, the ratio M_s/M is sequentially decreased in order to simulate variable source thickness scenarios. The numerical results (Figure 4.2) and their comparison with the analytical plume lengths obtained from eq. (4.6) clearly suggests that the latter will provide a good estimate, up to 2 times higher, for any $M_s/M > 50\%$. This result is also significant because, unlike the numerical approach, the analytical approach does not consider ED degradation from below the plume. Hence, the obtained results suggest that the ED degradation is dominantly controlled by degradation from the top in that range. Eq. (4.6) will result in higher overestimates, in the range of an order of magnitude, for $20\% < M_s/M < 50\%$. Further decreasing M_s/M eventually yields negative plume length, indicating that the simplification made to eq. (4.2) by considering only the first term of the infinite series is not valid in that range. Figure 4.2 also suggests that eq. (4.6) could be used to estimate plume length in very shallow (M <1 m) aquifers for any M_s/M ratio.

The inset in Figure 4.2 provides alternative approaches to evaluate eq. (4.6). For the first approach M_s is set equal to M. This makes eq. (4.6) identical to the 2D expression for a fully penetrating source provided in *Liedl et al.* (2005). The obtained results (for $M = 3$ m, log-scale and the plot with + symbol in the inset of Figure 4.2), after comparing with numerical results for partially penetrating sources, are qualitatively similar to the results obtained for the main plot in Figure 4.2. Quantitative differences are found significant only for $M_s/M < 50\%$. The obtained results suggest that the expression provided in *Liedl et al.* (2005) can also be used for sufficiently thicker sources. In addition, the results clearly identify that the degradation of the contaminant is controlled from the top for $M_s/M > 50\%$.

As a second alternative approach, the M is set equal to M_s in eq. (4.6). With this approach the analytical model is found to underestimate (in inset of Figure 4.2) the numerical plume for every selected M_s, clearly indicating that this approach

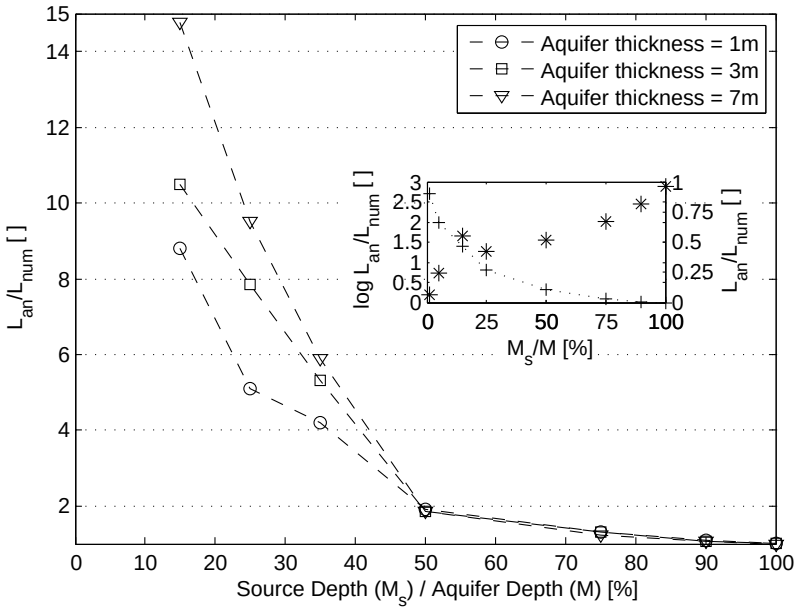

Figure 4.2: Comparing Numerical (L_{num}) and Analytical (L_{an}) plume lengths for different source thicknesses in a 2D domain. The inset plot (log-scale and with + symbol) compares L_{num} and L_{an} obtained from the expression provided in *Liedl et al.* (2005). The second plot in the inset compares L_{num} with L_{an} obtained from eq. (4.6) with M replaced by M_s for the 3 m deep aquifer.

should not be applied. Comparable results were obtained for the both approaches when aquifer depth was changed to 1 m and 7 m.

From the above analysis, it can be concluded that eq. (4.6) can be, in general, used for estimating plume lengths when the source thickness is above 25% of the aquifer depth. Expression provided in *Liedl et al.* (2005) can also be used for sufficiently thicker sources, but larger overestimates will result in that case. Numerical method is recommended for sources that are below 25% of the aquifer depth. In the next subsection the approach adopted for obtaining 2D results will be utilized in the 3D domain.

4.3.2 The 3D Case

Qualitatively the results of the 3D case are expected to be similar to those obtained for the 2D case discussed above. However, quantitative differences can result due to the finite source width that provides additional degradation surfaces for the ED. To verify, the Comsol Multiphysics® modeling environment is again used for the numerical experiments with the 3D domain. The numerical domain is set exactly

as in Figure 4.1. Including all parameters required for the 2D model, the 3D model additionally requires a finite source width ($2W$), the finite lateral domain width ($2W_D$) and the transverse horizontal dispersivity (α_{Th}) to be specified. W is always set to four times the aquifer thickness (M) in each direction from the center, i.e., $2W = 8M$. Likewise, W_D is also fixed and is always $2.5 * W$ in each lateral direction. α_{Th} is considered ten times larger than α_{Tv}, resulting in value of 50 cm. These parameters are fixed as we focus on source thickness in this chapter. The boundary conditions of the numerical domain are set in the following way: The planar ED source (M_s x $2W$) is set to a constant concentration boundary equaling to $\gamma * C_D = 3.5$ x 15 mg/L. The EA entering the domain from the top, from the lateral directions and from the parts of the inflow boundary not occupied by the source are also constant concentration boundaries with concentration $-C_A = -8$ mg/L. This concentration was also used at the outflow boundary.

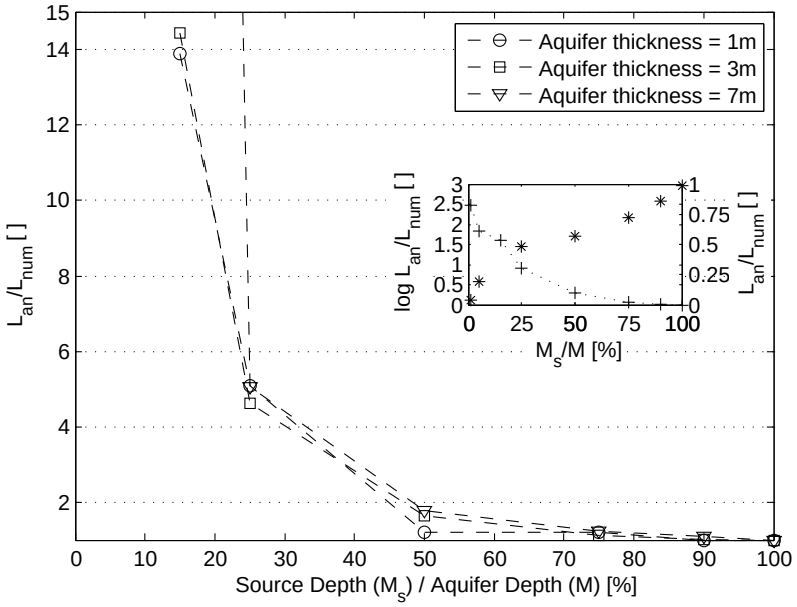

Figure 4.3: Comparing Numerical (L_{num}) and Analytical (L_{an}) plume lengths for different source thicknesses in a 3D domain. The inset plot (log-scale and with + symbol) compares L_{num} and L_{an} obtained from the expression provided in *Liedl et al.* (2011). The second plot in the inset compares L_{num} with L_{an} obtained from eq. (4.5) with M replaced by M_s for the 3 m deep aquifer.

Numerically computed plume lengths and their comparison with plume lengths obtained by iteratively solving eq. (4.5) is provided in Figure 4.3. Numerical and analytical plume lengths are equal for M_s/M=100%, providing evidence that the selected numerical method is capable of simulating the *Liedl et al.* (2011) 3D model

scenario. As was expected, the 3D results (main plot) did not provide information that is principally different from the 2D results. Figure 4.3 confirms for the 3D case that plume length can be obtained from eq. (5) if $Ms/M > 50\%$. It is important to mention that eq. (4.5) fails to converge for $M_s/M < 10\%$, which defines the limitation of simplifying eq. (4.3). As numerical simulations result in very short plumes when M_s/M <10%, the limitation of eq. (4.3) may not be of very high practical importance.

The inset in Figure 4.3 provides a similar comparison between the numerical and analytical plume lengths that were already made for the 2D case (subsection 4.3.1). The 3D results confirm the results already obtained from the 2D case. It has to be noted that the comparisons between the analytical and numerical results are made with a relative scale in Figure 4.2 and Figure 4.3. In an absolute scale the 2D and the 3D plume lengths differ significantly. The impacts of varying source geometry, and other parameters, on plume length (e.g., *Liedl et al.* (2011)) for the 3D case remain to be evaluated. With the numerical technique provided in this chapter, such evaluations can be largely simplified. However, they remain beyond the scope of this chapter.

4.4 Conclusions

This chapter provides the expressions for estimating plume length originating from the non-fully penetrating source. The derived expressions straightforwardly modify the plume length estimates provided in *Liedl et al.* (2005, 2011). The obtained results clearly demonstrate that the modified expressions can, in general, be used for the cases when the source thickness (M_s) is over 25% of the aquifer depth. Although very short and often non-practical plumes will emerge when $M_s < 25\%$, numerical techniques have to be used for evaluating these cases. It is also very important to note that this chapter provides a very simple numerical technique to solve a mixing controlled reaction of two reactants in the 2D and 3D domains. The provided numerical technique bears the potential of being applicable to more complex (transient conditions, heterogeneous aquifer, irregular source shape, more general boundary conditions etc.) scenarios than used in this chapter.

Chapter 5

Recommendations for Future Works

This thesis dealt with a single parameter, L_{max}, associated with the contaminated sites. L_{max} was considered as a parameter with a potential application for the management of the contaminated sites. Only analytical models involved with L_{max} estimation were considered in the thesis. Therefore, the results provided in this thesis share all limitations of the analytical models, e.g., considering homogeneous systems when the general subsurface is heterogeneous or considering a binary type single step contaminant degradation reactions when a reaction in subsurface almost always involves more than two compounds and are often catalyzed by microorganisms or other compounds. Fortunately, mostly these limitations lead to overestimations rather than underestimations of the actual L_{max} (see chapter 2), which can still be useful for many cases. Nevertheless, it is important to quantify how much overestimate can be still considered as a good estimate. This definitely is quite a complex task but before that can be attempted, several simpler tasks need to be accomplished. Based on knowledge and experiences gained from this thesis, the details that follow recommend tasks that can be helpful in achieving an overall goal on the management of contaminated sites.

5.1 Extensions of Analytical Models

Simple Extension of Analytical Models

The analytical models provided in this thesis, and also found in literature, are rather restricted in their applicability. To increase applicability, the 3D model provided in this thesis can be rather easily reformulated to fit to the two of the

following cases:

1. Considering transient plumes.
2. Solution for the maximum plume width (W_{max}).

Figure 1.2 in the introductory chapter (1) provided a very concise picture of different stages of the plume development. Steady-state condition at the contaminated sites often gets disrupted due to natural phenomena such as rains, floods. Although new steady-state will be soon reached, the extension of the plume before, during and after the disruption need to be tracked. In addition, being able to predict growing or shrinking plumes will enhance the applicability of the analytical models. This all will require time dependent L_{max}. The analytical model developed in Chapter 3 provides the possibility of including the time dependent concentration profile, thus providing also plumes not at the steady-state condition. It is highly recommended that this possibility be explored in future works.

L_{max} is undoubtedly a very important parameter for the risk assessment of a contaminated site, but W_{max} is equally important if a complete contamination area or A_{max}, which is often desired by the regulatory agencies, is required to be obtained. Furthermore, knowing the thickness of the plume, maximum volume of the contaminated area can be determined, which in turn can be used to estimate the cost of remediation. The analytical model developed in chapter 3 and also provided in *Liedl et al.* (2011) can be re-worked to obtain an expression for estimating W_{max}. Some key questions could be, for example, the position of W_{max}, how W_{max} is related to other parameters, notably to the source geometry, of the site.

Complex Extensions of Analytical Models

If analytical models are to be used for purposes beyond pre-assessment of contaminated sites, then their limitations need to be overcome. This will require some complex extensions to the analytical models available in the literature. Listed below are few of these complex extensions that are recommended for future works:

1. Multi-Species (at least more electron acceptors) degradations.
2. Complex reaction mechanisms.
3. Variable flow velocity, diffusion and dispersion coefficients.
4. Ultimately heterogeneous domain.

In general, reactions at the contaminated site involve three or more compounds, beside being catalyzed by microorganisms or other compounds, e.g., *Wiedemeier et al.* (1999). *Newell et al.* (1995) used a simple superposition technique, provided by *Borden and Bedient* (1986), to incorporate multi-species reaction case to the analytical model provided by *Domenico* (1987). Similar procedures are required to be attempted with newer analytical models, e.g., to *Liedl et al.* (2005) model. Attempts have been made to include complex reaction mechanisms. *Cirpka and Valocchi* (2007) and *Cirpka* (2010), for instance, included biokinetics. Simpler and robust models with complex reaction mechanisms should be attempted in future works. Likewise, for the further development, attempts should be made to incorporate variable flow, compound specific diffusion and dispersion and heterogeneous scenarios. Impacts of these cases on L_{max} are provided from numerical and experimental works by, e.g., *Werth et al.* (2006) who considered a simple heterogeneous domain, while *Chiogna et al.* (2010) experimentally showed compound specific dispersion in a homogeneous system.

5.2 Parameter Estimation and Uncertainty Analysis

In chapter 2, in which very recent contaminated site data were compiled and analyzed, it was found that for almost all sites dispersions - longitudinal (α_L) or transversal (α_{Tv} or α_{Th}), data were not available. Also, most often data on source geometry (thickness or width) were missing from the site investigations. While source geometry, which are likely to have a value in range of tens of centimeter to a meter (*Wiedemeier et al.*, 1999), can be relatively easy to measure, it is unlikely that any field, laboratory or even numerical investigation can quantify dispersions, which are reported to have values smaller than a millimeter (e.g., *Cirpka et al.*, 2005) with a good accuracy. As such, parameter estimation methods have to be applied in order to obtain missing parameters or in the case of dispersion to obtain a best estimate. The estimated parameter when used in the model may lead to uncertain results, e.g., *McNab and Dooher* (1998) . Therefore, for future works attempts should be made to develop simple, efficient and robust parameter estimations and uncertainty analysis techniques.

5.3 Laboratory and Field Experiments

While several analytical models have been proposed in recent years, very less effort has been put into verifying these models in field or even from laboratory

experiments. Most often only few numerical experiments are performed for any verification purpose, e.g., *Cirpka and Valocchi* (2007). Attempts to verify analytical models using field data were made in chapter 2, but they were few and inconclusive. More such efforts are recommended for future works. Apart from directly verifying analytical models, laboratory experiments need to be performed for quantifying parameters these models require. Laboratory efforts to quantify dispersion, e.g., several works of Cirpka and Grathwohl, e.g., *Cirpka et al.* (2005), *Klenk and Grathwohl* (2002), have been inconclusive. In addition, extremely few works (e.g., *Zhang et al.*, 2007) on quantifying source geometry, which has been found to be more sensitive for L_{max} quantification, are available in literature. It is important that future works focus on developing efficient laboratory and field techniques for quantifying parameters, especially source geometry and dispersion, that are required by analytical models.

Appendix 1

Table A.1: KORA data from hydrocarbon contaminates sites. $*$ = derived from lab value, † = avg. from different sites and ‡ = Gypsum leaching. $\star$ marked sites are selected for modeling exercise. NA = Not Available, ND= Not Detected

Site/Compound	**Aquifer Thickness**	**Plume Length**	**Hydraulic Conductivity**	**Electron Donor**	**Electron Acceptor**				Plume State	Chem. Group
					O_2	NO_3	SO_4	$Fe(II)$		
Unit	[m]	[m]	$*10^{-}3$ [m/s]	[mg/L]	[mg/L]					
Niedergörsdorf TL1 (Ethylbenzol)	5-12	<140*	0,01	0,709	<1	9-12	34-54	12-19	Stationary	
Niedergörsdorf TL1 (Toluol)	5-12	<90*	0,01	0,04	<1	9-12	34-54	12-19	Stationary	
*Niedergörsdorf TL1 (m/p-Xylol)	5-12	120	0,01	1,3	1	9-12	34-54	12-19	Stationary	
Niedergörsdorf TL2 (m/p-Xylol)	5-12	80-90	0,01	2,4	<2	<10	20-40	20-40	Uncertain	
Niedergörsdorf TL2 (o-Xylol)	5-12	50-60	0,01	1,4	<2	<10	20-40	20-40	Uncertain	
Niedergörsdorf TL2 (Ethylbenzol)	5-12	80-90	0,01	0,7	<2	<10	20-40	20-40	Uncertain	
Brand (Benzol)	50-100	120-150	0,01-0,1	0,25	<1	depleted	0-15	<110	Stationary (model)	
Brand (m,p-Xylol)	50-100	60-100	0,01-0,1	>0,4	<1	depleted	0-15	<110	Stationary (model)	BTEX
*OLES-Epple (DRM: BTEX)	5-15	160	0,02	0,31	<1	ND	<200	<2	Stationary	
OLES-Epple (BH:BTEX)	0,5-2	120	0,1	0.014	NA	NA	NA	NA	Stationary	
*VMZ Spandau 1.GWL (BTEX)	11	250	0,5	33	7,5*	0,5†	17†	NA	Shrinking	
*Castrop-Rauxel 1.Stockwerk (Benzol)	5-7,4	200	0,001-1	123	1.6	<1	120-1400‡	NA	Stationary (model)	
Gaswerk Düsseldorf (Toluol)	15-20	600	0,1-1	90	NA	NA	NA	NA	Non-stationary	
*Metlen (BTEX)	1,5-6	∼500	0,4-3	230	0,6	<5	650	0,3	Quasi Stationary	
Wülknitz (BTEX)	30	300	0,0001-3,2	0,4	NA	depleted	depleted	NA	Uncertain	

Continuation of Table A.1

Site/Compound	**Aquifer Thickness**	**Plume Length**	**Hydraulic Conductivity**	**Electron Donor**	**Electron Acceptor**				Plume State	Chem. Group
					O_2	NO_3	SO_4	$Fe(II)$		
Unit	[m]	[m]	$*10^{-3}$ [m/s]	[mg/L]	[mg/L]					
Niedergörsdorf TL1 (1,2,4-TMB)	5-12	<60*	0,01	1	<1	9-12	34-54	12-19	Stationary	
Niedergörsdorf TL1 (Ethyltoluol)	5-12	<100*	0,01	0,88	<1	9-12	34-54	12-19	Stationary	
Niedergörsdorf TL1 (1,2,3-TMB)	5-12	∼100	0,01	0,6	<1	9-12	34-54	12-19	Stationary	
Niedergörsdorf TL1 (1,3,5-TMB)	5-12	∼100	0,01	0,2	<1	9-12	34-54	12-19	Stationary	Other HC
Niedergörsdorf TL 2: (Cumol)	5-12	40	0,01	0,2	<2	<10	20-40	20-40	Uncertain	
Niedergörsdorf TL2 (Ethyltoluol)	5-12	60-65	0,01	0,13	<2	<10	20-40	20-40	Uncertain	
Brand (1,2,4-TMB)	50-100	60-100	0,01-0,1	0,25	<1	depleted	0-15	<110	Stationary (model)	
Brand (Ethyltoluol)	50-100	60-100	0,01-0,1	0,16	<1	depleted	0-15	<110	Stationary (model)	
Metlen (MTBE)	1,5-6	<2000	0,4-3	290	0,6	< 5	650	0,3	Quasi Stationary	
Castrop-Rauxel 1.Stockwerk (Naphthalin)	5-7,4	325	0,001-1	35	1.6	<1	120-1400‡	0,045	Growing (model)	
Castrop-Rauxel 1.Stockwerk (NSO-HET)	5-7,4	325	0,001-1	22	1.6	<1	120-1400‡	NA	NA	
Düsseldorf (Naphthalin)	15-20	600	0,1-1	10	NA	NA	NA	NA	Non-Stationary	
Testfeld Süd (Acenaphthen)	3,3	450	3-3,7	32	0,23	<1	<53	NA	NA	
Testfeld Sud (HET-Dimethylbenzofuran)	3,3	450	3-3,7	11.5	0,23	<1	<53	NA	NA	
Testfeld Sud (PAK ohne Naphthalin)	3,3	450	3-3,7	max 10	0,23	<1	<53	NA	NA	
OLES-Epple DRM (sum PAK)	5-15	160	0,02	1,2	<1	ND	<200	<2	Stationary	
OLES-Epple BH (sum PAK)	0,5-2	120	0,1	0.015	NA	NA	NA	NA	NA	
Wülknitz (NSO-HET Benzothiophen)	30	300	0,0001-3,2	<3	NA	depleted	depleted	NA	Uncertain	
Wülknitz (Naphthalin)	30	>300	0,0001-3,2	<10	NA	depleted	depleted	NA	Uncertain	PAK
Wülknitz (Acenaphthen)	30	>300	0,0001-3,2	0,6	NA	depleted	depleted	NA	Uncertain	
Wülknitz (Fluoren)	30	300	0,0001-3,2	∼0.2	NA	depleted	depleted	NA	Uncertain	
Wülknitz (Phenanthren)	30	300	0,0001-3,2	∼0,009	NA	depleted	depleted	NA	Uncertain	
Wülknitz (Pyren)	30	150	0,0001-3,2	0,001	NA	depleted	depleted	NA	Uncertain	
VMZ Spandau 1.GWL (sum PAK)	11	50	0,5	0,65	7,5*	NA	0,5†	17†	Shrinking	

Table A.2: KORA data from chlorinated solvents contaminated sites. Dispersivity values are from model results.

Sites/compounds	**Aquifer Thickness**	**Plume Length**	**Hydraulic Conductivity**	**Electron Donor**	**Longitudinal Dispersivity**	**Transverse Dispersivity**	
						Horizontal	**Vertial**
Unit	[m]	[m]	[m/s]	[mg/L]	[m]	[m]	[m]
Hannover (PCE)	15-20	>2000	0,0003-0,001	2	0,5	0,05	0,01
Karlruhe (PCE, TCE)	15-20	>2000	0,003	2,6			
Düsseldorf (Cl-Alkane, PCE)	10-24	4400	0,002	3,7	2,5-5	0,25-0,5	
Rosengarten (PCE)	>230∗	950∗	0,00001-0,00005	3,6		0,05	
Frankenthal (PCE, TCE)	7-18	1200	0,0001-0,0007	1,3	10	0,1	0,01
Perleberg (TCE)	5-24	200-300		62,3			

Appendix 2

Inversion Formula for the Heaviside function

An inversion formula has to be used in order to obtain a solution for b_n from eq. (3.7). A compilation of mathematical solutions by *Bronshtein and Semendyayev* (1997, p. 575, eq. 5) provides an expression for b_n, which is given as

$$\begin{aligned} b_n(0,y) &= \frac{2}{M}\int_0^M \big[H(y+W)-H(y-W)\big]\sin(2n-1)\frac{\pi z}{2M}\mathrm{dz} \qquad \text{(A-1)} \\ &= \frac{2}{M}\big[H(y+W)-H(y-W)\big]\int_0^M \sin(2n-1)\frac{\pi z}{2M}\mathrm{dz} \\ &= \frac{2}{M}\big[H(y+W)-H(y-W)\big]\big[-\frac{2M}{(2n-1)\pi}\cos(2\mathrm{n}-1)\frac{\pi \mathrm{z}}{2\mathrm{M}}\big]_0^{\mathrm{M}} \end{aligned}$$

Finally, we get eq. (3.8) by inserting the limits of integration, i.e,

$$b_n(0,y) = \frac{4}{\pi}\frac{1}{2n-1}\big[H(y+W)-H(y-W)\big]$$

Approach for the Numerical Calculation of the Plume Length

In order to numercally calculate the plume length with inclusion of all parameters, eq. (3.19) is rewritten as a function of L_1 as in

$$f(L_1) = \mathrm{erf}\frac{\mathrm{W}}{\sqrt{4\alpha_{\mathrm{Th}}\mathrm{L}_1}}\cdot \mathrm{e}^{-\alpha_{\mathrm{Tv}}\left(\frac{\pi}{2\mathrm{M}}\right)^2 \mathrm{L}_1} - \frac{\pi}{4}\frac{\gamma \mathrm{C}_{\mathrm{D}}^{\mathrm{thres}} + \mathrm{C}_{\mathrm{A}}^{\circ}}{\gamma \mathrm{C}_{\mathrm{D}}^{\circ} + \mathrm{C}_{\mathrm{A}}^{\circ}} \qquad \text{(A-2)}$$

Mathematical analysis reveals that $f(L_1)$ is monotonically decreasing with $f(0) > 0$ and $f(+\infty) < 0$, i.e., there must be exactly one zero. As f is differentiable with respect to L_1, the Newton Raphson (NR) method is assumed to be the best technique to obtain the solution. Finding an appropriate starting value for L_1 is the most important aspect in guaranteeing that the NR method converges

to the solution. This is achieved by assuming that the two factors in the first term on the right-hand side of eq. (A-2) are equal. In this case, each of them is identical to the square root of the chemical term, i.e.,

$$\mathrm{erf}\frac{\mathrm{W}}{\sqrt{4\alpha_{\mathrm{Th}}\mathrm{L}_1}} = \sqrt{\frac{\pi}{4}\frac{\gamma\mathrm{C}_{\mathrm{D}}^{\mathrm{thres}} + \mathrm{C}_{\mathrm{A}}^{\circ}}{\gamma\mathrm{C}_{\mathrm{D}}^{\circ} + \mathrm{C}_{\mathrm{A}}^{\circ}}} \tag{A-3}$$

and

$$e^{-\alpha_{Tv}\left(\frac{\pi}{2M}\right)^2 L_1} = \sqrt{\frac{\pi}{4}\frac{\gamma C_D^{thres} + C_A^{\circ}}{\gamma C_D^{\circ} + C_A^{\circ}}} \tag{A-4}$$

As eq. (A-3) cannot be directly solved for L_1, a very good approximate solution (accurate to within 1%) provided by *Williams* (1946) is taken. Solution for the first L_1 is obtained by setting $\mathrm{erf}(x) = \sqrt{1 - e^{-\frac{4}{\pi}x^2}}$ as in

$$1 - e^{-\frac{4}{\pi}\frac{W^2}{4\alpha_{Th}L_1}} = \frac{\pi}{4}\frac{\gamma C_D^{thres} + C_A^{\circ}}{\gamma C_D^{\circ} + C_A^{\circ}}$$

which upon simplifying and rearranging provides a solution for L_1 as

$$L_1 = -\frac{W^2}{\pi\alpha_{Th}\ln\left(1 - \frac{\pi}{4}\frac{\gamma C_D^{thres} + C_A^{\circ}}{\gamma C_D^{\circ} + C_A^{\circ}}\right)} \tag{A-5}$$

Likewise, rearranging eq. (A-4) provides a second solution for L_1 as

$$L_1 = -\frac{2}{\pi^2}\frac{M^2}{\alpha_{Tv}}\ln\left(\frac{\pi}{4}\frac{\gamma C_D^{thres} + C_A^{\circ}}{\gamma C_D^{\circ} + C_A^{\circ}}\right) \tag{A-6}$$

The smaller of the two L_1's obtained is used as starting value for L_1 in the NR iteration. This was because the curvature of f was found to be positive, thus indicating that "an approach from the left" ensures convergence due to the monotonically decreasing behavior. The solution routine provided above has been implemented in an Excel^{TM} spreadsheet.

References

Bajracharya, B. (2011), Exploring analytically and numerically the impact of source geometry, vertical source dimension and groundwater and contaminant chemistry on the development of contaminant plume, *M.Sc. thesis*, TU Dresden, Dresden, Germany. [in page nr. : 24]

Bauer R. D., M. Rolle, S. Bauer, C. Eberhardt, P. Grathwohl, O. Kolditz, R. U. Meckenstock, and C. Griebler (2009), Enhanced biodegradation by hydraulic heterogeneities in petroleum hydrocarbon plumes, *J. Contam. Hydrol., 105*(1–2), 56–68. [in page nr. : 25, 29]

Bear, J.(1979), Hydraulics of Groundwater, *McGraw-Hill*, NY. [in page nr. : 21]

Bear, J., and Cheng, A., (2008), Modeling Groundwater Flow and Contaminant Transport, *Springer*. [in page nr. : 5]

Bekins, B. A., E. Warren, and E. M. Godsy (1998), A comparison of zero-order, first order, and Monod biotransformation models, *Ground Water, 36*(2), 261–268. [in page nr. : 30]

Borden, R. C. and Bedient, P. B. (1986), Transport of dissolved hydrocarbons influenced by oxygen limited biodegradation: theoretical development, *Water Resour. Res., 22*(9), 1973–1982. [in page nr. : 18, 56]

Bronshtein, I. N., and K. A. Semendyayev (1997), *Handbook of mathematics*, 3rd ed., Springer, N.Y. [in page nr. : 35, 61]

Carslaw, H. S., and J. C. Jaeger (1959), *Conduction of heat in solids*, 2nd ed., Oxford Univ. Press, N.Y. [in page nr. : 35]

Chu, M., P. K. Kitanidis, and P. L. McCarty, (2005), Modeling microbial reactions at the plume fringe subject to transverse mixing in porous media: when can the rates of microbial reactions be assumed to be instantaneous?, *Water Resour. Res., 41*, Doi: 10.1029/2004WR003495. [in page nr. : 24, 30, 31, 46]

Cirpka, O. A., E. O. Frind, and R. Helmig (1999), Numerical simulation of biodegradation controlled by transverse mixing, *J. Contam. Hydrol., 40*(2), 159–182. [in page nr. : 29]

Cirpka, O. A. (2002), Choice of dispersion coefficient in reactive transport calculations on smooth fields, *J. Contam. Hydrol., 58*, 261–282. [in page nr. : 9, 30]

Cirpka, O. A., Å. Olsson, Q. Ju, M. A. Rahman, and P. Grathwohl (2006), Determination of transverse dispersion coefficients from reactive plume lengths, *Ground Water, 44*(2), 212–221. [in page nr. : 30, 31, 56, 57]

Cirpka, O., and A. Valocchi (2007), A two-dimensional concentration distribution for mixing-controlled bioreactive transport in steady state, *Adv. Water Resour., 30*, 1668–1679. [in page nr. : 25, 46, 56, 57]

Cirpka, O. (2010), Simplified simulation of steady state bioreactive transport with kinetic solute uptake by the biomass. *Water Resour. Res., 46*(7), 1-12. doi: 10.1029/2009WR008977. [in page nr. : 25, 46, 56]

Chiogna, G., C. Eberhardt, P. Grathwohl, O. Cirpka, and M. Rolle (2010), Evidence of compound-dependent hydrodynamic and mechanical transverse dispersion by multitracer laboratory experiments, *Environ. Sci. Technol., 44*(2), 688–693. [in page nr. : 34, 56]

Crank, J. (1976), *The mathematics of diffusion*, 2nd ed., Oxford Univ. Press, N.Y. [in page nr. : 36]

Domenico, P. A., and G. Robbins (1985), A new method of contaminant plume analysis, *Ground Water, 23*(5), 476–485. [in page nr. : 6, 20, 30]

Domenico, P. A. (1987), An analytical model for multidimensional transport of a decaying contaminant species, *J. Hydrol.,, 91*, 49–58. [in page nr. : 6, 20, 30, 56]

EPA (US Environmental Protection Agency) (1996), BIOSCREEN Natural attenuation decision support system, *No.: EPA/600/R-96/087*, @*ONLINE* November 22, 2012. URL: http://www.epa.gov/ada/csmos/models/bioscrn.html. [in page nr. : 21]

EPA (US Environmental Protection Agency) (1999), Use of monitored natural attenuation at superfund, RCRA corrective action, and underground storage tank sites, *Directive No.: 9200.4-17P*, Office of Solid Waste and Emergency Response, US EPA, USA. @*ONLINE* November 22, 2012. URL: http://www.epa.gov/oust/directiv/d9200417.pdf. [in page nr. : 2]

EPA (US Environmental Protection Agency) (2000), Innovative remediation technologies: field-scale demonstration projects in North America, 2nd Edition,*EPA 542-B-00-004*, Office of solid waste and emergency response, US EPA, USA. @*ONLINE* November 22, 2012. URL: http://http://www.clu-in.org/download/remed/nairt_2000.pdf. [in page nr. : 4]

Grajales, J. (2011), Evaluation of analytical models on plume length estimations using statistical analysis of large contaminant sites database, *M.Sc. thesis*, TU Dresden, Dresden, Germany. [in page nr. : 23, 25]

Grathwohl, P., I. D. Klenk, C. Eberhardt, and U. Maier (2001), Steady state plumes: Mechanism of transverse mixing in aquifers. In: New Approaches Characterizing Ground Water Flow, *A. A. Balkema* (Brookfield, Vt.): 89–93. [in page nr. : 9, 29, 30]

Gutierrez-Neri, M., P. Ham, R. Schotting, and D. Lerner (2009), Analytical modelling of fringe and core biodegradation in groundwater plumes, *J. Contam. Hydrol., 107*, 1–9. [in page nr. : 25, 31]

Guyonnet, D., and C. Neville (2004), Dimensionless analysis of two analytical solutions for 3-D solute transport in groundwater, *J. Contam. Hydrol., 75*, 141–153. [in page nr. : 21]

Ham, P. A. S., R. J. Schotting, H. Prommer, and G. B. Davis (2004), Effects of hydrodynamic dispersion on plume lengths for instantaneous bimolecular reactions, *Adv. Water Resour., 27*(9), 803–813. [in page nr. : 6, 22, 30, 31, 34, 37, 38, 46]

Huang, W., S. Oswald, D. Lerner, C. Smith, and C. Zheng (2003), Dissolved oxygen imaging in a porous medium to investigate biodegradation in a plume with limited electron acceptor supply, *Environ. Sci. Technol., 37*, 1905–1911. [in page nr. : 9, 22, 30]

Hunkeler, D., P. Höhener, and O. Atteia (2010), Comments on "Analytical modelling of fringe and core biodegradation in groundwater plumes." by Gutierrez-Neri et al. in J. Contam. Hydrol. 107: 1–9., *J. Contam. Hydrol., 117*, 1–6. [in page nr. : 25, 31]

Klenk, I. D., and P. Grathwohl, (2002), Transverse vertical dispersion in groundwater and the capillary fringe J. Contam. Hydrol. **58**, 111–128. [in page nr. : 57]

KORA TV-1, Wabbels, D., G. Teutsch, (2008), Leitfaden Natürliche Schadstoffminderungsprozesse bei mineralölkontaminierten Standorten Methoden, Empfehlungen und Hinweise zur Untersuchung und Beurteilung, KORA-Themenverbund 1 Raffinerien, Tanklager, Kraftstoffe/Mineralöl, MTBE.-@*ONLINE* November 22, 2012. URL: http://www.natural-attenuation.de/media/document/15_6949kora-tv1-leitfaden.pdf. [in page nr. : 11, 26]

KORA TV-2, Werner, P., P. Börke, N. Hüsers, (2008), Leitfaden Natürliche Schadstoffminderung bei Teerölaltlasten, KORA-Themenverbund 2 Gaswerke, Kokereien, Teerverarbeitung, (Holz-)Imprägnierung.- @*ONLINE* November 22, 2012. URL: http://www.natural-attenuation.de/media/document/15_6954kora-tv2-leitfaden.pdf. [in page nr. : 11]

KORA TV-3, Grandel,S., A. Dahmke, (2008), Leitfaden Natürliche Schadstoffminderungsprozesse bei LCKW-kontaminierten Standorten Methoden, Empfehlungen und Hinweise zur Untersuchung und Beurteilung, KORA Themenverband 3,Chemische Industrie, Metallverarbeitung.- @*ONLINE* November 22, 2012. URL: http://www.gpi.uni-kiel.de/Angewandte/angew_geo-Dateien/lftv3/. [in page nr. : 11]

Koussis, A., S. Pesmajoglou, and D. Syriopoulou (2003), Modelling biodegradation of hydrocarbons in aquifers: when is the use of the instantaneous reaction approximation justified? *J. Contam. Hydrol., 60*(3-4), 287–305. [in page nr. : 30]

LABO (Bund/Länder-Arbeitsgemeinschaft Bodenschutz) (2009), Berücksichtigung der natürlichen Schadstoffminderung bei der Altlastenbearbeitung, *Positionpapier.: 10.12.2009*, Ministerium für Umwelt, Forsten und Verbraucherschutz des Landes Rheinland-Pfalz, Germany. @*ONLINE* November 22, 2012. URL: http://www.labo-deutschland.de/documents/MNA-Positionspapier_Stand_10-12-2009_e51.pdf. [in page nr. : 3, 8]

Liedl, R., A. J. Valocchi, P. Dietrich, and P. Grathwohl (2005), Finiteness of steady state plumes, *Water Resour. Res., 41*, Wqw501, doi: 10.1029/2005WR004000. [in page nr. : xvii, 6, 9, 22, 23, 30, 31, 34, 35, 37, 38, 39, 44, 45, 46, 48, 49, 50, 51, 53, 56]

Liedl, R., P. K. Yadav., and P. Dietrich, (2011), Length of 3D mixing-controlled plumes for a fully penetrating contaminant source with finite width, *Water Resour. Res., 47*, W08602, doi: 10.1029/2010WR009710. [in page nr. : xvii, 6, 24, 46, 48, 49, 50, 52, 53, 55]

Lyman, W.J., W. F. Reehl, and D. H. Rosenblatt, (1982), Adsorption coefficients for soils and sediments, *In: Handbook of Chemical Property Estimation Methods*, McGraw-Hill, New York. [in page nr. : 17, 18]

Maier, U., and P. Grathwohl (2006), Numerical experiments and field results on the size of steady state plumes, *J. Contam. Hydrol., 85*(1–2), 33–52. [in page nr. : 24, 31, 38]

Martian, P., K. S. Sorenson, and L. N. Peterson (2003), A critique of the internal tracer method for estimating contamination degradation rates, *Ground Water, 41*(6), 632–639. [in page nr. : 30]

Mayer, K.U., (1999), A multicomponent reactive transport model for variably saturated media, Department of Earth Sciences. *PhD Thesis.,*, University of Waterloo, Ontario, Canada. [in page nr. : 5]

McNab, W. W., and B. P. Dooher (1998), Critique of a steady-state analytical method for estimating contaminant degradation rates, *Ground Water, 36*(7), 983–987. [in page nr. : 30, 56]

Monod, J. (1942), The Growth Of Bacterial Cultures (La croissance des cultures recherches sur la croissance des cultures bacteriennes), Hermann and Cie, Paris, France [in page nr. : 19]

Newell, C. J., L. P. Hopkins, and P. B. Bedient (1990), A hydrogeologic database for groundwater modeling, *Ground Water 28*, 703–714. [in page nr. : 12]

Newell, C. J., J. W. Winters, H. S. Rifai, R. N. Miller, J. Gonzalez, and T. H. Wiedemeier (1995), Modeling intrinsic remediation with multiple electron acceptors: results from seven sites, *Nationa Ground water Association (NGWA)-Proceeding of the petroleum hydrocarbon and organic chemicals in ground water conference*, Houston, Texas, USA, November 1995, 33–48. [in page nr. : 10, 21, 56]

Norris, R. D. (1995), In-Situ Bioremediation of Ground Water and Geological Material : A Review of Technologies, *Diane Publishing Company*, Darby, PA. [in page nr. : 9]

Olsson, Å., M. Piepenbrink, and P. Grathwohl (2004), Determination of transverse dispersivities at lab scale: Conservative transport and steady state reactive plumes, *Geophys. Res. Abstr.,* Abstract 06712. [in page nr. : 30]

Prokop, G., M. Schamann and I. Edelgaard (2000), Management of contaminated sites in Western Europe, *Topic report No.: 13/1999*, European Environmental Agency. [in page nr. : 1, 9]

Prommer, H., Barry, D. A., and Davis, G. B. (2002), Modeling of physical and reactive processes during biodegradation of a hydrocarbon plume under transient groundwater flow conditions, *J. Contam. Hydrol., 59*(1–2), 113–131. [in page nr. : 30]

Prommer H, D. A. Barry, and C. Zheng, (2003), MODFLOW/MT3DMS-based reactive multicomponent transport modelling, *Ground Water., 41*(2), 247–57. [in page nr. : 5]

Rice, D. W., R. D. Grose, J. C. Michaelsen, B. P. Dooher, D. H. MacQueen, S. J. Cullen, W. E. Kastenberg, L. G. Everett, and M. Marino (1995), California Leaking Underground Fuel Tank (LUFT) historical case analyses, *California State Water Resources Control Board*, CA, USA [in page nr. : 12, 14, 28]

Rugner H and G. Teutsch (2001), Literature study, Natural attenuation of organic pollutants in groundwater, Integrated Concept for Groundwater Remediation (INCORE) -Final Report, *Contract No.: EVK1-CT-1999-00017*, Center of Applied Geosciences, University of Tübingen. [in page nr. : xvi, 3, 4]

Srinivasan, V., T. P. Clement, and K. K. Lee (2007), Domenico solution–is it valid?, *Ground Water 45*(2), 136–146. [in page nr. : 22]

Teutsch, G., P. Grathwohl, and T. Schiedek (1997), Literaturstudie zum natrlichen rückhalt / abbau von schadstoffen im grundwasser, *Technical Rep. Texte und Berichte zur Altlastenbearbeitung 35/97*, Landesanstalt Für Umweltschutz Baden-Württemberg, Karlsruhe, Germany. [in page nr. : 10, 12, 28, 29, 30, 41]

Thullner, M., L. Mauclaire, H. Schroth, W. Kinzelbach, and J. Zeyer (2002), Interaction between water flow and spatial distribution of microbial growth in a two-dimensional flow field in saturated porous media, *J. Contam. Hydrol., 58*, 169–189. [in page nr. : 2, 9, 30]

U.S. National Research Council (2000), *Natural Attenuation for Ground Water Remediation*, Natl. Acad. Press, Washington, D. C. [in page nr. : 30]

Werth, C. J., O.A. Cirpka, and P. Grathwohl (2006), Enhanced mixing and reaction through flow focusing in heterogeneous porous media, *Water Resour. Res., 42*, W12414, doi: 10.1029/2005WR004511. [in page nr. : 29, 31, 56]

Wexler. E. J. (1992), Analytical solutions for one-, two-, and three-dimensional solute transport in ground-water flow systems with uniform flow, US Geological Survey, *Applications of hydraulics, chapter B7.* @*ONLINE* November 22, 2012. URL: `http://pubs.usgs.gov/twri/twri3-b7/pdf/TWRI_3-B7.pdf`. [in page nr. : 6, 10, 15]

Williams, J. D. (1946), An Approximation to the Probability Integral, *The Annals of Mathematical Statistics, 17*(3), 363–365. [in page nr. : 62]

Wiedemeier, T., H. Rifai, C. Newell, J. Wilson (1999), Natural Attenuation of Fuels and Chlorinated Solvents in the Subsurface, *John Wiley*, New Jersey. [in page nr. : 2, 8, 10, 12, 13, 14, 16, 21, 22, 23, 29, 30, 31, 33, 39, 40, 48, 56]

Yadav, P. K., Händel, F., Müller, C., Liedl, R., and P. Dietrich, (2011), A Simulation tool for analytical estimation of plume length, *In revision in Grundwasser* [in page nr. : 25]

Yadav, P. K., Liedl, R., and P. Dietrich, (2012), Influence of Source Thickness on Steady-State Plume Length, *submitted to Water Resour. Res.* [in page nr. : 24]

Zhang, C., C. J. Werth, and A. G. Webb, (2007), Characterization of NAPL source zone architecture and dissolution kinetics in heterogeneous porous media using magnetic resonance imaging, *Environ. Sci. Technol., 41*(10), 3672–3678. [in page nr. : 57]

Zheng, C., and G. D. Bennett (2002), *Applied Contaminant Transport Modeling*, John Wiley, NY. [in page nr. : 5, 44]